Diversification of small RNA pathways underlies germline RNAi incompetence in wild *C. elegans* strains

Han Ting Chou[1], Francisco Valencia[1], Jacqueline C. Alexander[1], Avery Davis Bell[1], Diptodip Deb[1], Daniel A. Pollard[2], Annalise B. Paaby[1,3]

1. School of Biological Sciences, Georgia Institute of Technology, Atlanta, GA, USA
2. Biology Department, Western Washington University, Bellingham, WA, USA
3. Correspondence: paaby@gatech.edu

ABSTRACT

The discovery that experimental delivery of dsRNA can induce gene silencing at target genes revolutionized genetics research, by both uncovering essential biological processes and creating new tools for developmental geneticists. However, the efficacy of exogenous RNAi varies dramatically within the *C. elegans* population, raising questions about our understanding of RNAi in the lab relative to its activity and significance in nature. Here, we investigate why some wild-type strains fail to mount a robust RNAi response to germline targets. We observe diversity in mechanism: in some strains, the response is stochastic, either on or off among individuals, while in others the response is consistent but delayed. Increased activity of the Argonaute PPW-1, which is required for germline RNAi in the laboratory strain N2, rescues the response in some strains, but dampens it further in others. Among wild-type strains, genes known to mediate RNAi exhibited very high expression variation relative to other genes in the genome as well as allelic divergence and strain-specific instances of pseudogenization at the sequence level. Our results demonstrate functional diversification in the small RNA pathways in *C. elegans*, and suggest that RNAi processes are evolving rapidly and dynamically in nature.

INTRODUCTION

In *C. elegans*, the landscape of molecular and developmental genetics was transformed by the ability to silence genes by feeding worms *E. coli* bacteria engineered to express RNA matching worm gene targets (*Kamath et al., 2003; Rual et al., 2004; Timmons & Fire, 1998*). This tool emerged from the seminal discovery that double stranded RNA induces gene suppression (*Fire et al., 1998*). Awarded the Nobel prize in 2006, the discovery launched research into new mechanisms of gene regulation and led to characterization of the microRNA (miRNA), short interfering RNA (siRNA), and PIWI-interacting (piRNA) pathways. These pathways overlap in gene set and molecular mechanisms, but mediate processes as diverse as cell growth and tissue differentiation, adaptive immunity against pathogens, transgenerational epigenetic inheritance, and germline defense against transposons (*Grishok, 2013; Wilson & Doudna, 2013*). Decades of investigation have illuminated a complex meta-phenomenon, with distinct sub-processes including the regulation of transcriptional silencing in the nucleus versus post-transcriptional silencing in the cytoplasm, of endogenous biogenesis of the small RNA trigger versus exogenous or environmental delivery, of local versus systemic responses, and of silencing genes in the soma versus targets in the germline. These processes are all captured under the umbrella term "RNA interference" (RNAi), the general mechanism of gene silencing via dsRNA (*Yigit et al., 2006*). Many of the genes that encode RNAi machinery are shared across plants, animals, and fungi, and appear deeply conserved within the eukaryotic lineage (*Shabalina & Koonin, 2008; Wynant et al., 2017*).

However, even as *C. elegans* sits at the epicenter of expansive research programs into gene silencing by small RNAs, wild-type strains vary significantly in capacity for RNAi. The universal laboratory strain N2 is robustly sensitive to RNAi, but its competence is not representative (*Félix, 2008*). For example, RNAi against germline targets in 55 wild isolates revealed a quantitative range of responses, from negligible to more sensitive than N2 *(Paaby et al., 2015*). Wild-type strains also vary in competence for targets in the soma, and some strains show incompetence for RNAi by both feeding and injection (*Félix et al., 2011; Paaby et al., 2015; Tijsterman et al., 2002*). To date, the only causal variant identified for natural differences in RNAi is a frameshift lesion in the Argonaute *ppw-1*, which partially explains germline RNAi

insensitivity in the Hawaiian isolate CB4856 (*Tijsterman et al., 2002*). The genetics underlying differences in RNAi efficacy in *C. elegans* are otherwise unknown.

RNAi silences complementary mRNA targets via the association of small RNAs with Argonaute effector proteins (*Wilson & Doudna, 2013*). The Argonaute superfamily includes the ancient AGO proteins; the PIWI Argonautes, which are conserved in animals; and in *C. elegans*, the WAGO proteins, an expanded clade of Argonautes specific to nematodes (*Youngman & Claycomb, 2014*). The expansion of Argonautes signifies a critical role for RNAi in nematodes, and has been hypothesized to underlie the extraordinary diversification of worms across environments, perhaps having enabled adaptations associated with environmental sensing, parasitism, and immunity (*Buck & Blaxter, 2013*). Likewise, the momentum of discovery of RNAi-associated phenomena at the bench increasingly indicates that gene regulation by small RNAs dominates *C. elegans* biology (*Houri-Zeevi et al., 2020; Youngman & Claycomb, 2014*).

Given the evident importance of RNAi in *C. elegans*, why is its efficacy so variable? Here, we investigate the genetic basis of germline RNAi deficiency in wild *C. elegans* strains. We aim to elucidate how the response fails in incompetent strains, the role of *ppw-1*, and whether the genetic architecture of incompetence is simple or complex. We also evaluate expression and allelic diversity at genes known to mediate RNAi, to compare RNAi responses at the organismal level to proximate causes of failure. These analyses uncover evidence of extensive diversification of RNAi activity within *C. elegans*, consistent with rapid and recent evolution of a genetically complex trait. This level of functional variability in RNAi pathways offers a useful access point into connecting the vast body of *C. elegans* RNAi research to the biological relevance of these processes in nature.

RESULTS

Germline RNAi varies in expressivity and penetrance over reproductive age and among genotypes

Prior work examining embryonic gene knockdown in wild *C. elegans* demonstrated that strains vary quantitatively in the strength of their germline RNAi response, and that strains CB4856 and

90 QX1211 appear largely incompetent for germline RNAi (*Paaby et al., 2015*). In contrast, the
91 common wild-type laboratory strain N2 is highly sensitive to RNAi, though germline RNAi can
92 be eliminated in N2 with a deletion at the WAGO Argonaute *ppw-1* (*Tijsterman et al., 2002; Yigit*
93 *et al., 2006*). To directly compare RNAi incompetence in the N2 mutant ($N2^{ppw\text{-}1(del)}$), CB4856,
94 and QX1211, we targeted the maternal-effect, embryonic-required genes *par-1* and *pos-1*, which
95 have commonly been used to measure germline RNAi (*Elvin et al., 2011; Pollard & Rockman,*
96 *2013; Tijsterman et al., 2002*). We fed worms *E. coli* expressing target dsRNA, then counted dead
97 embryos in the next generation. Under a conventional approach of pooling worms on plates and
98 scoring offspring in a window of relatively early egg-laying (*Kamath et al., 2001; Pollard &*
99 *Rockman, 2013*), our observations were consistent with prior reports: wild-type N2 exhibited high
100 lethality, and the three incompetent strains exhibited very low or negligible lethality (Figure 1A).
101
102 However, following an initial trigger, amplification within the RNAi response can induce strong
103 effects later (*Billi et al., 2014*), and continual exposure to RNAi by feeding also means that
104 individuals ingest increasing numbers of trigger molecules as they age. To evaluate whether the
105 response changes over time within individual animals, we scored the penetrance of embryonic
106 lethality over the complete reproductive lifespan of egg-laying individuals. In this assay we
107 targeted *par-1*, which provides the more sensitive readout since it is not as lethal. Here, each of
108 the three incompetent strains exhibited a distinct response, indicating differences in genetic
109 mechanism (Figure 1B).
110
111 N2 showed complete lethality in all but the earliest offspring, suggesting that in this sensitive
112 strain, early amplification of the initial trigger rapidly induces total gene knockdown. In the
113 mutant $N2^{ppw\text{-}1(del)}$, however, nearly all embryos hatched, including late-age embryos (Figure 1B),
114 indicating that the loss of *ppw-1* is not compensated by other genes in the N2 background.
115
116 In CB4856, hermaphrodite mothers exhibited no evidence of an RNAi response in the first half
117 of their reproductive lifespan, but embryonic lethality emerged in the second half and increased
118 with parental age (Figure 1B). This suggests that the mutation in *ppw-1*—which encodes a
119 frameshift and early stop upstream of the critical PAZ and PIWI domains and is putatively
120 responsible for insensitivity in CB4856 (*Elvin et al., 2011; Pollard & Rockman, 2013; Tijsterman et*
121 *al., 2002*)—is either not a null allele and permits some PPW-1 activity, or that other genes in the

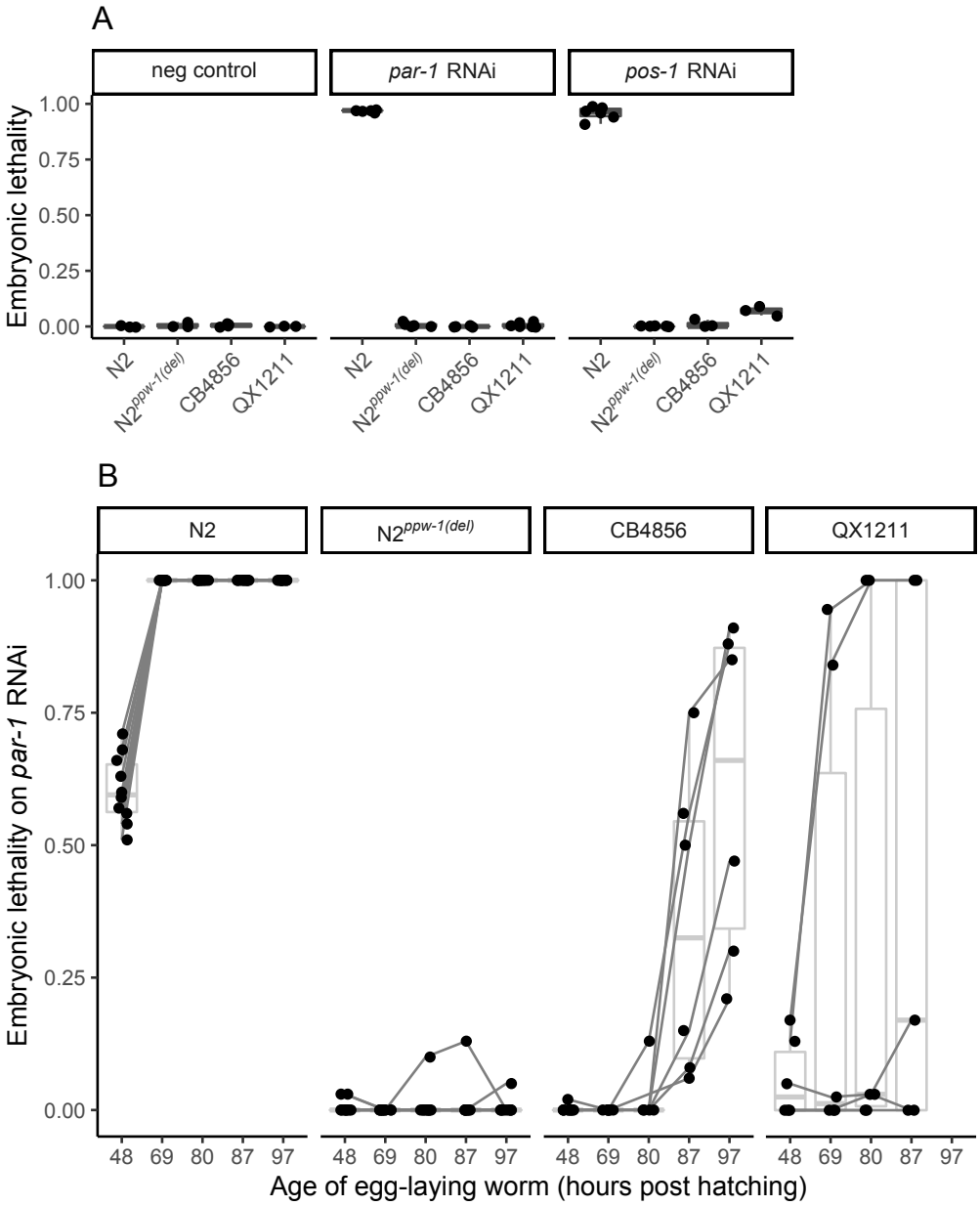

Figure 1. Embryonic lethality following RNAi against germline-expressed targets. (A) Hatched larvae and dead embryos laid in a 4-6hr window within the first 8hrs of egg-laying were scored for pooled hermaphrodites across replicate plates. (B) To assess the germline RNAi response over reproductive lifespan, embryonic lethality was scored for individuals. Each point represents the proportion of dead embryos, out of total laid on a plate by a single hermaphrodite, in the given time interval. The data include all offspring of all hermaphrodite mothers; time intervals were chosen to space out the number of offspring per plate (~30-100); x-axis labels indicate the approximate midpoint of the time intervals. Connecting lines indicate the sequence of offspring plates for each individual. Embryonic lethality for all strains on the negative control empty vector was negligible (data not shown).

133 CB4856 background partially compensate for the loss of PPW-1, promoting a delayed RNAi
134 response.
135
136 QX1211 exhibited a third unique non-competent response. After a short delay, embryonic
137 lethality was either negligible or complete, suggesting that RNAi in QX1211 is either "on" or
138 "off" in individual animals (Figure 1B). Thus, unlike N2$^{ppw\text{-}1(del)}$, in which the RNAi response
139 appears abolished, CB4856 and QX1211 do exhibit limited responses, but with distinct patterns
140 of activity: in CB4856, the response is delayed and incomplete; in QX1211, it is partially
141 delayed, with higher expressivity and variable penetrance.
142
143 These results point to distinct differences in the execution of germline RNAi within *C. elegans*.
144 However, the use of an end-point phenotype to read out the RNAi response, i.e. embryonic
145 lethality, does not capture activity at the molecular or cellular level. Moreover, variation in the
146 *par-1* pathway between strains might influence phenotypic expression, confounding
147 interpretation of the RNAi response (*Paaby et al., 2015*). Therefore, we developed an assay to
148 measure the expression and knockdown of the target gene directly.
149
150 **Target transcript knockdown confirms distinct RNAi responses across strains**
151
152 To assess the RNAi response with high spatial and temporal resolution within embryos, we used
153 single-molecule fluorescence *in situ* hybridization (smFISH) to visualize transcripts of germline
154 RNAi targets. Since smFISH visualizes individual molecules via hybridization of dozens of
155 oligonucleotide probes, which in aggregate produce a detectable fluorescent spot (*Raj et al.,*
156 *2008*), it captures signals from intact RNAs, not those degraded by RNAi. These experiments
157 confirmed that the distinct responses of CB4856 and QX1211 are driven by variation in RNAi
158 mechanism, not in developmental variation related to the RNAi target. They also illustrated
159 consistent transcript degradation across the early stages of embryogenesis.
160
161 We examined *par-1* transcript levels in *par-1* RNAi-treated and -untreated embryos of N2,
162 CB4856 and QX1211. We collected embryos from gravid worms in early reproductive maturity,
163 in a narrow two-hour window, to maximize precision in estimating the RNAi response. At this
164 timepoint, many *par-1* transcripts are degraded in RNAi-treated N2 embryos (Figure 2A-B).

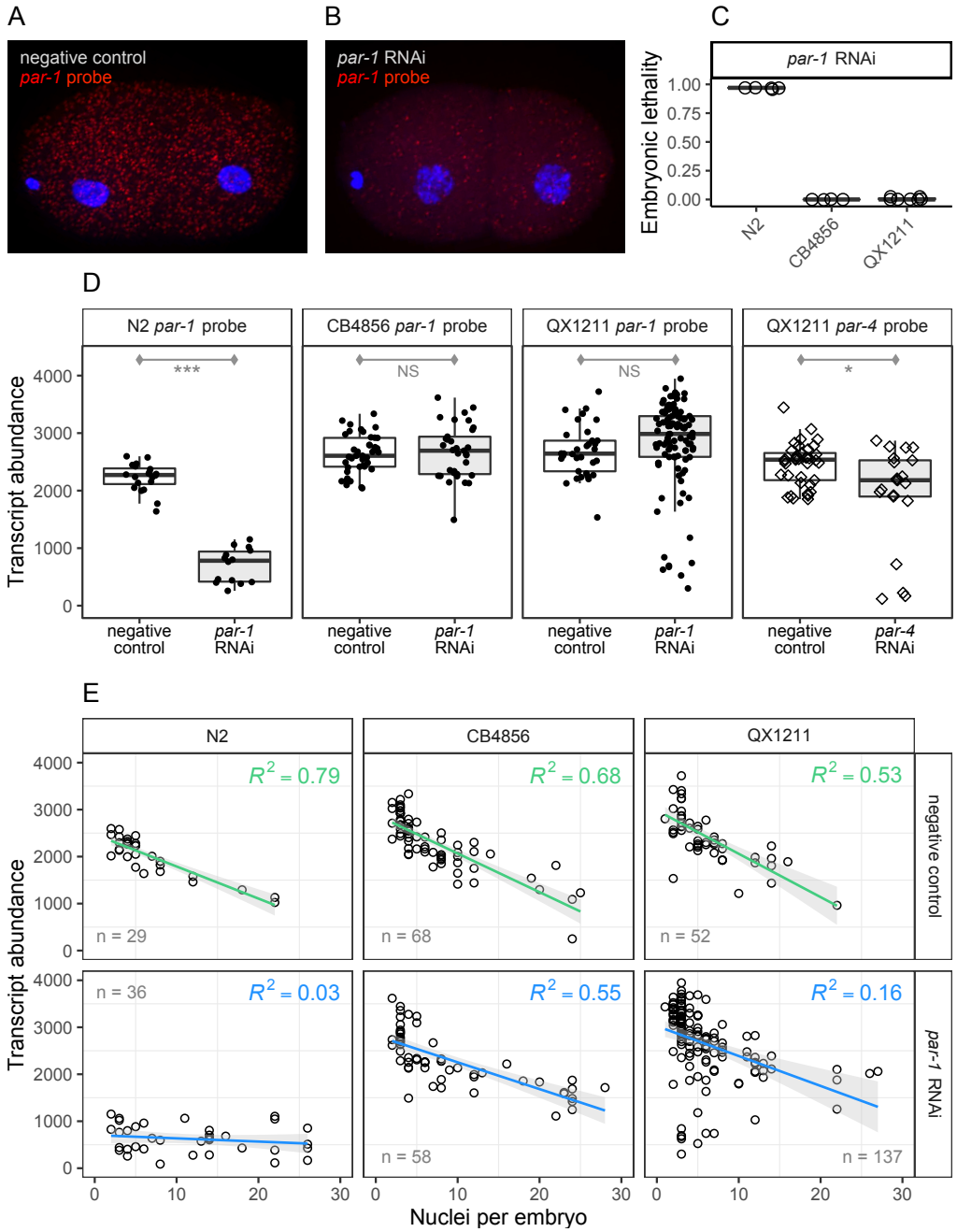

Figure 2. Transcript abundance in individual RNAi-treated and untreated embryos, visualized via single-molecule fluorescence in situ hybridization (smFISH). (A) - (B) Representative embryos are shown from strain N2, from a mother reared in the control condition or with RNAi against *par-1*; red spots indicate *par-1* transcripts and blue DAPI staining shows nuclei, which were used to identify embryo stage. (C) Embryonic lethality was simultaneously measured in matched samples. To limit variation due to reproductive age of the mothers, we collected embryos from a tightly controlled time window in early reproduction. (D) Transcript abundance for early stage embryos (up to four cells). (E) Transcript abundance for *par-1* for the same experiment, but now including later stage embryos with up to 30 nuclei. Green (negative control) and blue (RNAi treatment) lines indicate the linear regression of transcript counts onto embryonic stage; gray shading indicates the 90% confidence interval. For (D) and (E), each point represents one embryo. Significance levels (*t*-tests): $p<0.001$ (***), $p<0.01$ (**), $p<0.05$ (*).

178 Treated N2 embryos of this timepoint go on to show complete lethality, but in CB4856 and
179 QX1211, lethality is not yet penetrant (Figure 2C).
180
181 All three strains displayed robust expression of the target gene in untreated embryos (Figure 2D),
182 indicating that levels of native gene expression are unlikely to be a major influence on lethality
183 penetrance. However, in RNAi-treated embryos, N2 showed a steep drop in transcript
184 abundance, CB4856 showed no change, and QX1211 showed an on/off pattern with N2-like
185 levels for some, but not most, embryos. This pattern in QX1211 was replicated for a second
186 target, *par-4* (Figure 2D); see File S1 for statistical details. Thus, the patterns of transcript
187 knockdown following RNAi are highly consistent with our prior observations of strain-specific
188 responses.
189
190 To examine how transcript abundance, with and without degradation by RNAi, changes with
191 embryonic development, we evaluated embryos with up to 30 nuclei. In the control condition,
192 *par-1* transcripts decreased with embryonic stage (Figure 2E) (*Charles et al., 2021*) at a consistent
193 rate across strains (ANCOVA model comparison, $p=0.299$), indicating no apparent differences in
194 *par-1* developmental activity. In the treatment condition, the strain-specific patterns of transcript
195 degradation persisted without any apparent effect of development on the RNAi response (Figure
196 2E). That is, the treated N2 embryos, following a significant knockdown in transcript number
197 ($p<0.001$), exhibited a flat slope that implies no change in RNAi response with embryo stage.
198 The treated CB4856 and QX1211 embryos exhibited negligible change by embryo stage relative
199 to the control condition, with marginal ($\omega^2=0.017$, $p=0.012$) and non-significant changes in
200 slope, respectively. (The complete statistical report for this analysis, including estimates of the
201 variance explained and significance levels for ANCOVA model comparisons, is in Table S1.)
202 Thus, in this narrow window of embryogenesis and among embryos retrieved from a fixed-age
203 parent, we find no evidence of changing rate of degradation by embryo stage.
204
205 **Reduced PPW-1 function does not universally explain loss of germline RNAi**
206
207 Given the distinct patterns of germline RNAi incompetence in CB4856 and QX1211, we next
208 sought to evaluate the genetic basis for RNAi failure in these and other low-response strains.
209 First, we first considered the role of *ppw-1*. The naturally-occurring frameshift mutation in *ppw-*

210 *1* (*Tijsterman et al., 2002*) is unique to CB4856 in the *Caenorhabditis elegans* Natural Diversity
211 Resource (CeNDR) database (*Cook et al., 2017*), but we hypothesized that variation in PPW-1
212 activity arising from other sources might contribute to variation in germline RNAi among wild
213 strains. To test whether reduction of PPW-1 function is a universal aspect of reduced germline
214 RNAi, we performed complementation tests by crossing N2 wild-type and null alleles of *ppw-1*
215 to seven wild isolates. We evaluated CB4856, QX1211, and five additional strains, selected
216 based on prior observations of weak germline RNAi (data not shown) (*Paaby et al., 2015*) and
217 representation of nucleotide diversity and divergence across the global population (*Cook et al.,*
218 *2017*).
219
220 We crossed each wild isolate to N2 with its native, wild-type copy of *ppw-1*, and also to N2
221 carrying the *ppw-1* deletion allele (*pk1425*). Two genetic incompatibilities segregating within *C.*
222 *elegans* (*Ben-David et al., 2017; Seidel et al., 2008, 2011*) complicated our crosses, one of which we
223 controlled with a knockout allele at *peel-1*; details are provided in File S2. For each cross, we
224 compared the response of the individual wild isolate to the two heterozygote genotypes in the F1
225 generation, with and without the deletion at *ppw-1* inherited from the N2 chromosome. We
226 reasoned: though N2 homozygous for the *ppw-1* deletion fails to exhibit an RNAi response, one
227 copy of wild-type *ppw-1* fully rescues it, indicating that *ppw-1* is haplo-sufficient, at least in the
228 N2 background (Figure 3A). Therefore, if weak RNAi in the wild strains is a consequence of
229 reduced PPW-1 activity, any restoration of response in the F1 genotypes should be greater in the
230 genotype with the functional N2 *ppw-1* allele. As previously, we induced *par-1* RNAi in the (F1)
231 parent germline and measured embryonic lethality in the following generation. To avoid
232 confounding differences in developmental timing with variation in RNAi response, we scored all
233 progeny from only the first 15hrs of egg-laying from a small pool of hermaphrodite parents
234 (~100-200 embryos) on each replicate plate.
235
236 The seven strains exhibited four distinct response patterns: (i) no rescue, (ii) *ppw-1*-dependent
237 rescue, (iii) *ppw-1*-dependent suppression, and (iv) *ppw-1*-independent rescue, described in detail
238 below. These results indicate that within *C. elegans*, PPW-1 activity varies, PPW-1 activity
239 differentially affects germline RNAi due to interaction with other varying factors, or both. The
240 results further suggest that weak germline RNAi is multigenic within each strain, since rescued
241 responses were all lower than N2 levels, indicating the presence of factors other than *ppw-1*.

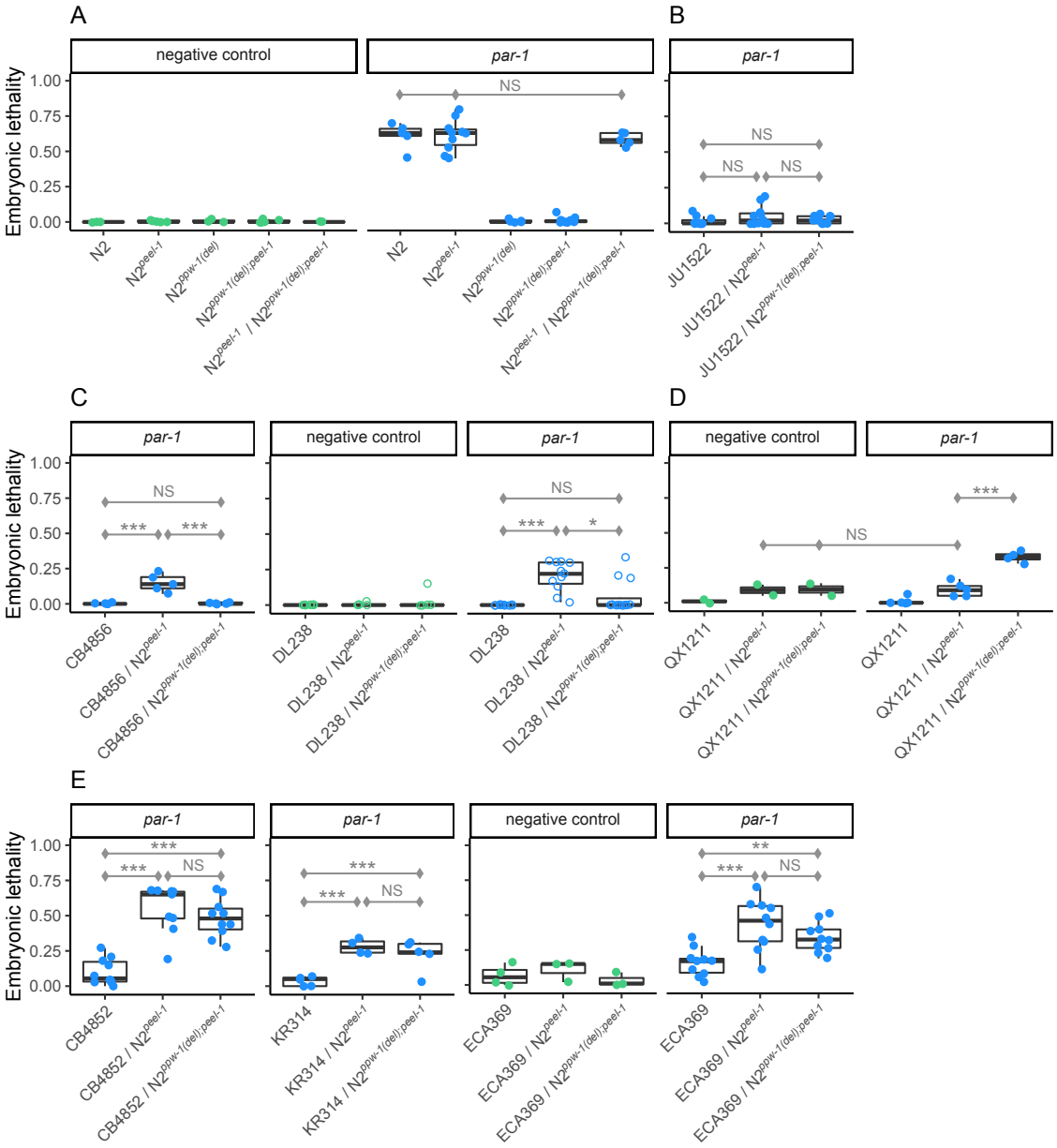

Figure 3. Complementation tests between seven wild isolates with low RNAi response and the RNAi-sensitive laboratory strain N2, with and without the *ppw-1* deletion allele. Response was measured by embryonic lethality following RNAi by feeding against the embryonic target *par-1*. Points represent the average across pooled hermaphrodites, with one exception (see below). (A) To circumvent embryonic lethality arising from the *zeel-1;peel-1* genetic incompatibility (*Seidel et al., 2008, 2011*), we used a null allele of the sperm-delivered toxin *peel-1* in N2, which has no effect on RNAi in either the responsive (N2) or the resistant ($N2^{ppw\text{-}1(del)}$) backgrounds. A single copy of *ppw-1* is sufficient to fully restore the germline RNAi response in N2. (B) - (E) Complementation tests for seven wild isolates with weak germline RNAi, representing a diversity of genetic backgrounds. Embryonic lethality in the control condition is shown when it was observed to be greater than zero. For DL238 (C), the open circles represent the proportion of dead embryos per individual; the overall pattern qualitatively replicates that which we observed in pooled hermaphrodites (Figure S2; individuals shown here to highlight variability). For QX1211 (D), the *sup-35;pha-1* incompatibility (*Ben-David et al., 2017*) induced embryonic lethality, visible in the control condition and the genotype without the *ppw-1* deletion in the *par-1* treatment (see File S1 for details). Significance levels (Tukey's contrasts): $p<0.001$ (***), $p<0.01$ (**), $p<0.05$ (*).

259 (i) Strain JU1522 showed no rescue, i.e., no improved RNAi response in either F1 genotype
260 (Figure 3B). This suggests that weak RNAi in JU1522 is independent of *ppw-1*, or at least that
261 alleles that promote RNAi in N2, including *ppw-1*, are not haplo-sufficient to increase the
262 response in the JU1522 background.
263
264 (ii) Strains CB4856 and DL238 exhibited *ppw-1*-dependent rescue: an increased RNAi response
265 when crossed to N2, but only in the background with the wild-type *ppw-1* allele (Figure 3C,
266 Figure S2). This outcome in CB4856 is consistent with prior reports (*Pollard & Rockman, 2013;*
267 *Tijsterman et al., 2002*). In DL238, replicate to replicate variation in embryonic lethality was high,
268 so we investigated whether this could be explained by potentially stochastic induction of the
269 RNAi response between individual worms. This appears to be the case: tested individually, some
270 hermaphrodites produced no dead embryos and others over 30% (Figure 3C).
271
272 (iii) Unexpectedly, QX1211 showed *ppw-1*-dependent suppression: the heterozygote with the
273 *ppw-1* deletion allele exhibited a significant increase in embryonic lethality, implying that
274 reduction of *ppw-1* in this strain promotes germline RNAi (Figure 3D). As expected in this cross,
275 we also observed lethality arising from the genetic incompatibility at the *sup-35;pha-1* locus
276 (*Ben-David et al., 2017*) (details in File S2).
277
278 (iv) Strains CB4852, KR314, and ECA369 exhibited *ppw-1*-independent rescue, in which the
279 two heterozygote genotypes exhibited levels of embryonic lethality that were equivalent to each
280 other and significantly higher than the wild isolate on its own. This suggests that N2 alleles other
281 than *ppw-1* promote the RNAi response in these genetic backgrounds (Figure 3E).
282
283 To ensure that differences in lethality came from variation in RNAi genes and not from
284 developmental variation specific to *par-1* (*Paaby et al., 2015*), we introgressed a germline-
285 expressed GFP construct into four strains representing the four observed response patterns and
286 quantified fluorescence following RNAi against GFP. With the exception of ECA369, which
287 showed higher than expected RNAi sensitivity, the responses confirmed RNAi incompetency
288 (Figure S3).

289 The results of these complementation tests demonstrate diversity in the function or effect of
290 PPW-1 activity within *C. elegans*. Further, the *ppw-1*-independent rescue and the incompleteness
291 of the *ppw-1*-dependent rescue implicate functional variation at genes other than (or in addition
292 to) *ppw-1*, indicating that wild-type strains are likely to carry mutations affecting RNAi at
293 multiple genes. However, with the exception of the unique *ppw-1* frameshift in CB4856, the
294 extent to which RNAi alleles are likely to be strain-specific, versus shared across the population,
295 is unclear.
296
297 **Genetic complementation between wild isolates implicates diverse and polygenic basis for**
298 **germline RNAi incompetence**
299
300 To examine whether alleles limiting germline RNAi are shared across strains, we crossed low-
301 response strains to each other and looked for complementation. As above, we measured
302 embryonic lethality following *par-1* RNAi exposure in the F1 generation. We performed a total
303 of six tests, with each pairwise cross for strains CB4856, DL238, KR314 and QX1211 (Figure
304 4), chosen based on their diversity in PPW-1 function (Figure 3) and compatibility at the *zeel-*
305 *1*;*peel-1* locus (*Andersen et al., 2012*) (see File S2 for more details).
306
307 We observed multiple instances of complementation, indicating that variation in RNAi is
308 polygenic and that low-response strains carry alleles with distinct functional effects. For
309 example, in the CB4856 × QX1211 cross, the heterozygote produced significantly more dead
310 embryos than either strain on its own (Figure 4A), indicating that alleles that dampen the RNAi
311 response are not shared since their function is at least partially rescued by the alternate genetic
312 background. Given that CB4856 and QX1211 exhibit responses that are dependent on *ppw-1* but
313 opposite to each other (Figure 3), their complementation may be occurring at *ppw-1* itself.
314 However, despite similar responses under *ppw-1* manipulation (Figure 3), DL238 and CB4856
315 also complement (Figure 4B), suggesting distinct mechanisms. DL238 failed to complement
316 QX1211 (Figure 4C), but did complement KR314 (Figure 4D), indicating shared and distinct
317 mechanisms, respectively; these outcomes are the opposite of those observed for CB4856
318 crossed to the same strains (Figure 4A, 4E), reinforcing the conclusion that CB4856 and DL238
319 harbor distinct genetic mechanisms. We also saw evidence for distinct mechanisms in the
320 complementation of KR314 × QX1211 (Figure 4F).

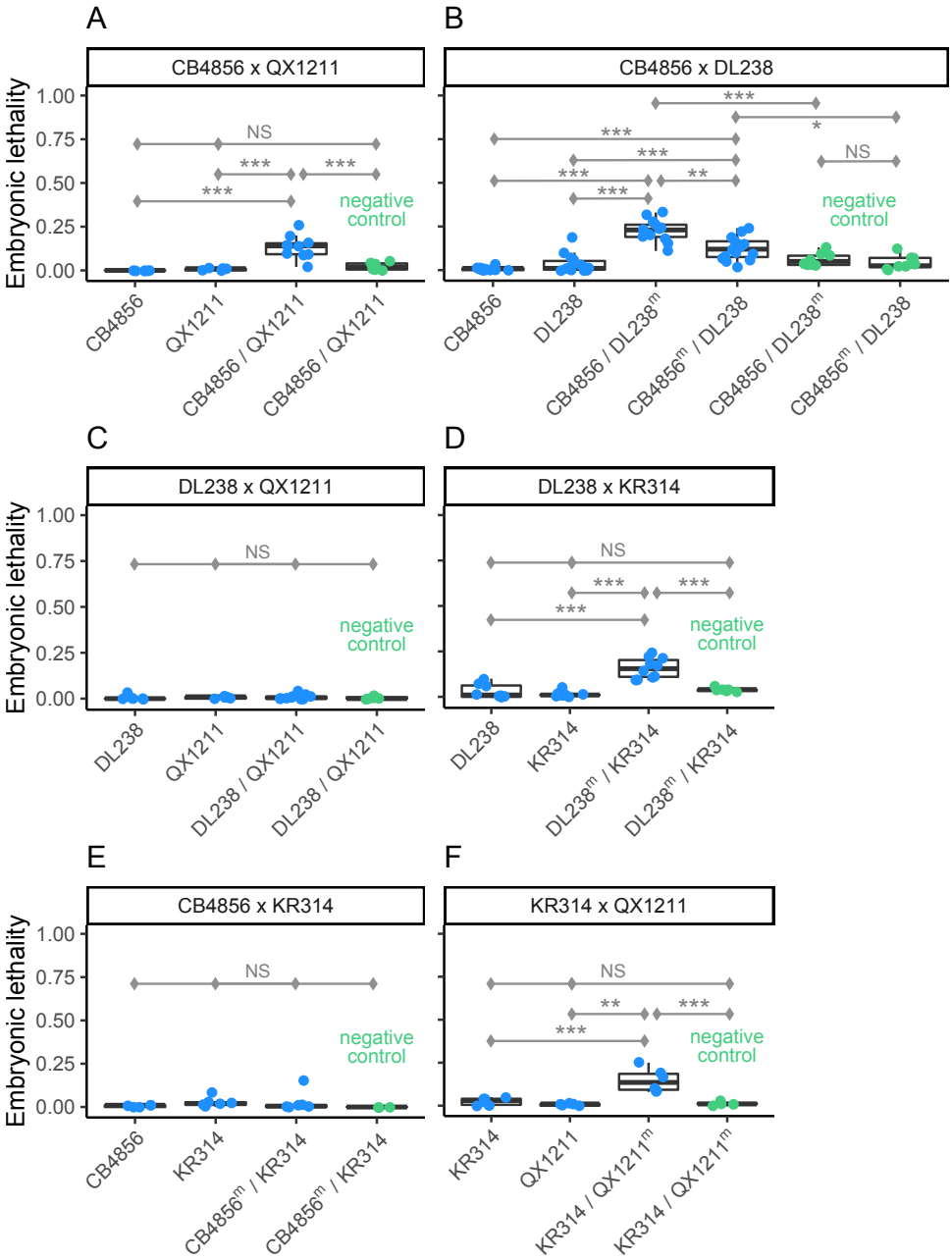

Figure 4. Pairwise complementation tests between four wild isolates with low RNAi response. (A) - (F) Response was measured by embryonic lethality following RNAi by feeding against the embryonic target *par-1*. The heterozygote genotypes were generated by crossing males and hermaphrodites in both directions (A) - (C), except for crosses with strain KR314, which does not produce fertile males (D) - (F). With the exception of CB4856 × DL238 (B), in which hermaphrodites sired by DL238 exhibited a significantly stronger response than those sired by CB4856, cross direction had no effect on embryonic lethality in the next generation and plots show pooled data. Significance levels (Tukey's contrasts): $p<0.001$ (***), $p<0.01$ (**), $p<0.05$ (*).

The rescued responses of the crossed strains point to pervasive diversity in the genetic mechanisms that underlie germline RNAi response in *C. elegans*. Together, the two sets of complementation assays (Figure 3, Figure 4) demonstrate that RNAi incompetence is multigenic within individual strains and caused by diverse alleles with distinct functional effects. This in turn indicates that variation in RNAi is a polygenic phenomenon within *C. elegans*, and suggests that it may be mediated by rare variants. In addition to *ppw-1*, causal mutations may reside in other Argonautes: though *ppw-1* is essential for germline RNAi in N2, overexpression of other WAGOs can rescue the response, implicating interchangeability (*Yigit et al., 2006*). We hypothesize that natural variation in the expression or function of RNAi genes, specifically WAGOs, produces a phenomenon of gene regulation by small RNAs that is highly diversified within the species. Variability in multiple factors is consistent with the dramatic range in sensitivity to germline RNAi overall (*Paaby et al., 2015*) as well as the diversity in genetic mechanisms underlying incompetence observed here.

C. elegans RNAi genes show unusually high variation in expression

To assess whether and how RNAi genes might vary in expression across strains, we performed RNA-seq on low-response strains CB4856 and QX1211, on responsive strains N2 and JU1088, and on strain EG4348, which shows an intermediate response (*Paaby et al., 2015*). RNA samples were prepared from young, reproductively mature hermaphrodites without RNAi induction. Relative to other genes in the genome, RNAi genes, in particular Argonautes, showed highly elevated expression variation across strains, including *ppw-1* and the related WAGO *sago-2*.

First, we examined expression at 62 genes known to directly mediate RNAi (listed in Table 1), including Argonautes currently classified as pseudogenes on Wormbase (*Harris et al., 2020*). Of these, all but two were expressed in every strain: *wago-5* was not expressed at all, and the putative pseudogene *ZK218.8* was not expressed in the responsive stains but was expressed in CB4856 and QX1211. Of the genes with detectable transcripts, approximately half (29/61) exhibited differential expression (FDR<0.1) between N2 and at least one other wild strain (Figure 5A).

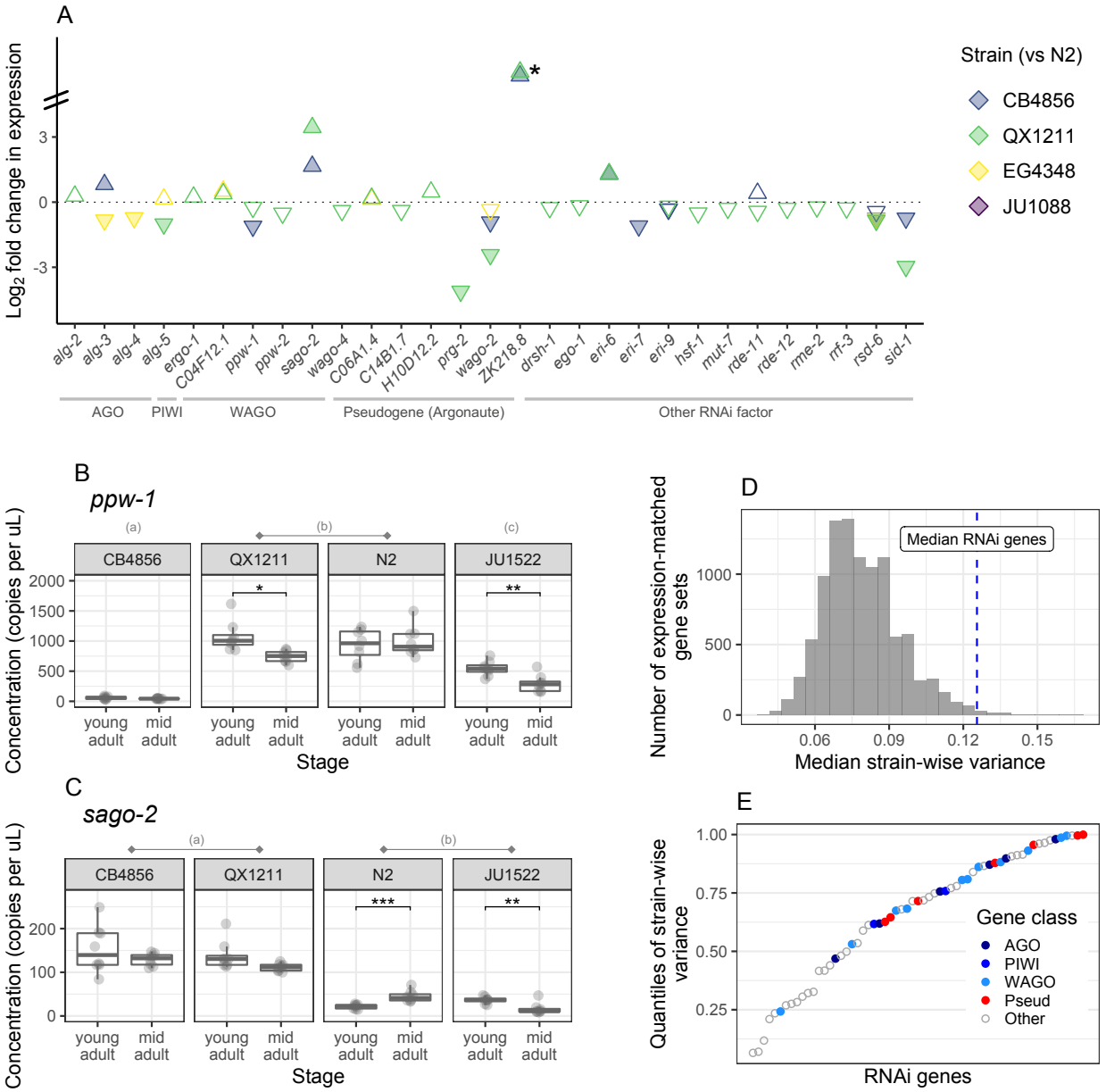

Figure 5. Variation in gene expression for RNAi factors. (A) Via RNA-seq, we examined 62 genes for differential expression between N2 and low-response strains CB4856 and QX1211, high-response strain JU1088, and moderately responsive strain EG4348. Only genes with significant results (FDR<0.1) are displayed; filled arrows indicate fold change >1.5. The (*) at *ZK218.8* indicates differential expression beyond the y-axis scale; this gene is not expressed in the N2 reference strain and has been classified as a pseudogene. (B) - (C) Expression differences via droplet digital PCR for *ppw-1* and *sago-2*. Ten strains were evaluated (Figure S4); a subset are shown here. Across strains, significant differences (Tukey's contrasts, p<0.05) are indicated by letter groupings; for example, QX1211and N2 have equivalent concentrations of *ppw-1*, while CB4856 and JU1522 concentrations are significantly different from all others. Within each strain, significant differences between developmental stages (pairwise contrasts with Bonferroni correction) are indicated by: p<0.001 (***), p<0.01 (**), p<0.05 (*). (D) Histogram of median strain-wise variance for 10,000 gene sets, expression-matched to the RNAi genes, randomly sampled across the genome following variance-stabilizing transformation. (E) Strain-wise variance of the 61 expressed RNAi genes, plotted by quantile of genome-wide variances (gene expression data as in D). Argonautes, including those currently classified as pseudogenes, are indicated by filled circles.

377 The strains with greatest differential expression were those with weakest germline RNAi (Figure
378 5A). That is: QX1211, then CB4856, showed the most differences across the gene set (26/61 and
379 10/61); the moderately responsive strain EG4348 showed a handful of differences (7/61); and the
380 highly responsive strain JU1088 showed a difference at only one gene (*rsd-6*) (Figure 5A). Of
381 genes differentially expressed by both CB4856 and QX1211, the direction of expression was
382 concordant with one exception (*rde-11*), including reduced expression of *ppw-1* and elevated
383 expression of *sago-2*. It is critical to note that though QX1211 and CB4856 show the greatest
384 degree of differential expression relative to N2, they are also the most genetically diverged (*Cook*
385 *et al., 2017*). That said, RNAi incompetence does not appear to be a function of genetic distance
386 from the reference strain, as highly diverged isolates ECA701, JU561, and XZ1516 (*Crombie et*
387 *al., 2019*) were responsive to *par-1* RNAi (data not shown), and RNAi sensitivity for 55 wild
388 isolates in (*Paaby et al., 2015*) showed no relationship with divergence from N2 (Figure S4).
389
390 The WAGO *sago-2* shares high sequence identity with *ppw-1* and resides ~17cM away on
391 chromosome I. These two genes share overlapping function in the N2 background (*Yigit et al.,*
392 *2006*), so the underexpression of *ppw-1* and overexpression of *sago-2* in CB4856 and QX1211
393 (Figure 5A) caught our attention. However, in some strains, including QX1211, poor mapping of
394 short reads to the reference genome (*Cook et al., 2017*) at these loci suggests gene divergence or
395 duplication. We resolved sequence ambiguities via de novo assembly of paired-end reads and
396 long read sequencing, and observed that QX1211 carries *ppw-1*-like alleles at both loci (File S3).
397 Therefore, to confirm our RNA-seq observations of *ppw-1* and *sago-2* expression and also to
398 evaluate additional strains, we designed a droplet digital PCR (ddPCR) experiment to measure
399 both transcripts simultaneously and discriminate between them using transcript-specific labels.
400 We tested all strains thus far discussed: the seven low-response strains for which we tested *ppw-*
401 *1* function (Figure 3), as well as responsive strains N2, JU1088, and EG4348. To evaluate
402 whether *ppw-1* or *sago-2* expression changed as worms aged, we also assayed two
403 developmental timepoints, young adult and mid adult.
404
405 The ddPCR results were consistent with our RNA-seq observations, and in sum confirm high
406 variability in *ppw-1* and *sago-2* expression (Figure 5B-C, Figure S5). Overall, *ppw-1* expression
407 was about an order of magnitude greater than that of *sago-2*, and both expression levels and
408 changes in expression between developmental timepoints differed significantly across strains for

409 both genes (Table S2). Taken individually, neither *ppw-1* nor *sago-2* expression correlated with
410 RNAi responsiveness, and across all ten strains, the combined expression was both highest and
411 lowest in two strongly resistant strains: QX1211 and JU1522, respectively (Figure 5B-C, Figure
412 S5). JU1522 has consistently exhibited negligible germline RNAi, including no rescue when
413 crossed with N2 (Figure 3) and no response even at later age (Figure S3); this strain shows the
414 weakest response we have observed. One possibility is that both high and low expression of *ppw-*
415 *1* and *sago-2* limit germline RNAi. This hypothesis fits with our observation that a haploid dose
416 of *ppw-1* increases the RNAi response in QX1211 (Figure 3D), and with the prior finding that
417 *ppw-1* and *sago-2* encode functionally interchangeable proteins that can compensate each other
418 (*Yigit et al., 2006*). However, it is inconsistent with the observation that overexpression of these
419 factors increases RNAi sensitivity in N2 (*Yigit et al., 2006*). N2 and JU1088, the two strains with
420 the most robust germline RNAi response in our analysis, exhibited intermediate levels of *ppw-1*
421 and *sago-2* combined (Figure S5).
422
423 Having observed significant expression variation for many of the RNAi genes, we next asked
424 whether this gene set is more variable than other genes in the genome. The answer is yes: for the
425 61 actively transcribed RNAi genes, the median strain-wise variance (after variance-stabilizing
426 transformation, see Methods) was higher than that of expression-matched sets randomly sampled
427 from the genome 99% of the time (9936/10,000 comparisons, Figure 5D); 74% of these
428 (7351/10,000) were statistically significant (one-tailed Mann-Whitney test, alpha=0.05), far
429 exceeding that expected by chance. This effect is driven by elevated variance across the gene set,
430 not by a few outliers of high variance, as the majority (57%) (35/61) exhibit significant
431 differences by strain via liklihood ratio test (FDR<0.1) compared to 29% of all genes in the
432 genome. Thus, RNAi genes are highly enriched for strain-wise variation ($p=4.8x10^{-6}$,
433 hypergeometric test).
434
435 Several of the RNAi genes are exceptionally variable. The putatively pseudogenized Argonaute
436 *prg-2* exhibits the 10th highest strain-wise variance in the genome, and six genes, including *ppw-*
437 *1* and *sago-2*, are in the top 2%. Given the relatively recent evolution of WAGOs (*Buck &*
438 *Blaxter, 2013*) and their potential redundancy in function (*Yigit et al., 2006*), we expected to see
439 especially high expression variation for this gene class. This hypothesis is well supported: all but
440 one (*sago-1*) of the 12 WAGOs are in the top half of genome-wide variance, though Argonautes

441 of all classes showed a similar trend, including those presumed to be pseudogenes (Figure 5E).
442 The distribution of strain-wise variances was more evenly distributed for other RNAi factors and
443 included both highly variable and highly invariant expression patterns (Figure 5E).
444
445 The elevated expression variation in RNAi genes represents heritable variation in small RNA
446 processes in *C. elegans*, consistent with the other evidence for diversification of germline RNAi
447 function within the species and a possible explanation for that diversity. Variable expression of
448 putative pseudogenes, including the active transcription of *ZK218.8* in some non-reference
449 strains, also prompts the question of whether wild-type strains vary in their complement of
450 functional Argonautes. *ZK218.8* was previously identified as an Argonaute (*Yigit, 2007*) but
451 remains unexplored in the literature; its expression signature suggests that pseudogenization may
452 have occurred in some strain lineages but not in others. While these observations all point to
453 diversification in genetic mechanisms of RNAi, the historical forces driving these outcomes
454 remain obscured. To evaluate this, and to look for evidence of strain-specific mutations affecting
455 RNAi, we next turned to population-level sequence data.
456
457 ***C. elegans* RNAi genes show lineage-specific diversification and pseudogenization**
458
459 We examined allelic diversity at the 62 RNAi genes, both to identify candidate mutations for
460 RNAi incompetence and to assess selection history via patterns of molecular variation. We
461 examined genotypes in CeNDR, which includes hundreds of strains representing the global *C.*
462 *elegans* population (*Cook et al., 2017*). For the seven low-response strains tested in the lab, we
463 identified putatively deleterious variants that may contribute to individualized loss of function, as
464 many were strain-specific (Table S3). Across the population, we observed substantial sequence
465 variation among all gene classes, including strain-specific instances of pseudogenization and
466 allelic divergence (Table 1). These results indicate that many RNAi genes have recently
467 undergone rapid and dynamic evolution, by what appears to be both relaxed and intense selection
468 pressure. The occurrence of rare alleles and lineage-specific patterns support the functional
469 diversification we observe in the lab and support a model of dynamic contemporaneous
470 evolution of small RNA pathways in *C. elegans*.

Table 1. Molecular diversity at 62 RNAi genes, from 403 strain isotypes. Genes were manually curated from the literature and include 20 putatively functional Argonautes and seven currently classified as pseudogenes on Wormbase (*Harris et al., 2020*), though pseudogene status varies in the literature (and likely across strains). "Functional diverged alleles" are those with at least 1% nucleotide divergence from the reference genome, including at least five moderate mutations, such as amino acid substitutions, and no disruptive high impact mutations, such as frameshifts or stop-gains. "Pseudogenized alleles" are those with at least one high impact mutation called with high confidence and at which 1% or more of the sites are diverged or missing, or those with at least 50% of the sites with missing calls. Potential pseudogenization was assessed with respect to the reference genome and considered even for those Argonautes already classified as putative pseudogenes.

Class	Gene	Nucleotide diversity (π)	No. strains with functional diverged alleles	No. strains with pseudo-genized alleles
Argonaute (AGO)	*alg-1*	7.20E-04	0	0
	alg-2	8.53E-04	0	19
	alg-3	6.86E-04	0	1
	alg-4	6.08E-04	10	5
	alg-5	3.75E-04	0	0
	rde-1	4.98E-04	2	0
Argonaute (PIWI)	*ergo-1*	1.18E-03	0	8
	prg-1	1.77E-03	0	0
Argonaute (WAGO)	*C04F12.1*	2.50E-04	0	34
	csr-1	6.59E-04	0	0
	hrde-1	1.84E-04	4	3
	nrde-3	3.39E-04	22	0
	ppw-1	2.77E-04	0	2
	ppw-2	5.35E-04	0	0
	sago-1	1.23E-03	0	4
	sago-2	1.26E-03	1	25
	wago-1	9.37E-04	0	0
	wago-10	9.64E-06	58	2
	wago-4	7.70E-06	0	0
	wago-5	9.17E-06	0	48
Argonaute (pseudo)	*C06A1.4*	1.07E-03	0	0
	C14B1.7	6.47E-04	0	0
	H10D12.2	3.00E-04	0	25
	prg-2	6.59E-04	0	3
	wago-11	7.58E-05	0	64
	wago-2	7.78E-04	0	0
	ZK218.8	4.08E-04	0	11
Other RNAi factor	*dcr-1*	6.37E-04	49	0
	drh-1	2.35E-04	40	0
	drsh-1	1.11E-03	0	0
	ego-1	1.07E-04	0	0
Other RNAi factor	*eri-1*	2.37E-04	23	0
	eri-12	5.00E-04	23	0
	eri-3	4.37E-04	9	0
	eri-5	7.15E-04	0	1
	eri-6	6.04E-04	36	20
	eri-7	1.74E-04	0	12
	eri-9	7.00E-04	26	0
	hrde-2	9.92E-04	0	0
	hsf-1	5.54E-03	119	0
	lin-15b	2.61E-04	9	53
	mut-7	8.90E-04	0	0
	nck-1	5.01E-04	0	0
	nhl-2	2.22E-04	0	0
	nyn-2	4.47E-04	2	1
	rde-10	1.00E-03	21	1
	rde-11	5.45E-05	0	1
	rde-12	2.46E-03	54	0
	rde-2	1.48E-04	0	0
	rde-4	7.21E-04	0	0
	rde-8	5.03E-06	0	0
	rme-2	2.09E-04	0	0
	rrf-1	1.09E-03	9	0
	rrf-3	1.19E-03	14	0
	rsd-2	2.67E-03	151	4
	rsd-3	2.00E-04	35	0
	rsd-6	2.68E-04	28	0
	sid-1	9.03E-04	0	1
	sid-2	1.44E-03	54	3
	sid-3	2.09E-04	56	1
	sid-5	1.23E-03	0	0
	tofu-5	6.59E-04	0	0

Relative to genome-wide averages (*Lee et al., 2021*), estimates of nucleotide diversity (π) per gene were generally high (Table 1), with π>0.001 for 14/62 genes (13/55 genes not characterized as pseudogenes). Elevated variation was often, but not always, associated with high-impact mutations in one or more strains (Figure S6). Therefore, to distinguish between instances of pseudogenization and gene loss versus functional allelic diversification arising from directional

488 or balancing selection, we classified highly diverged alleles two ways. We considered an allele to
489 be pseudogenized if it harbored at least one high impact mutation called with high confidence
490 and if at least 1% of the sites were diverged or missing relative to the reference genome, or if
491 over 50% of sites were missed calls; we classified "functional diverged alleles" as those with at
492 least five amino acid substitutions, at least 1% divergence across sites, and no high impact
493 mutations called at the locus.
494
495 We observed extensive pseudogenization across the gene set. Given the expansion and
496 diversification of Argonautes in nematodes (*Buck & Blaxter, 2013*), we hypothesized that the
497 WAGOs might be relatively unconstrained and therefore especially susceptible to gene loss.
498 Indeed, many WAGOs (7/13) showed evidence of pseudogenization, but putative loss occurred
499 in all gene classes, including the PIWIs, AGOs, and other RNAi factors (Table 1). For example,
500 the PIWI Argonaute *ergo-1* exhibits extensive variation and lineage-specific pseudogenization,
501 indicative of relaxed selection (Figure 6A). Excluding the seven Argonautes classified as
502 pseudogenes on Wormbase (*Harris et al., 2020*), 40% (22/55) of genes indicated pseudogenization
503 in one or more strains (Table 1). In contrast, a few genes exhibited very low polymorphism
504 (Figure 6B, Figure S6), likely reflecting evolutionary constraint and purifying selection. These
505 genes were mostly non-Argonautes, with the exception of *csr-1* and *prg-1*, the only Argonautes
506 essential for development (*Yigit et al., 2006*).
507
508 We also observed pervasive functional divergence, with functionally diverged alleles in 25/62
509 genes (Table 1). Unlike the pseudogenized alleles, which often occurred singly, the functional
510 diverged alleles were most often shared across strains, consistent with positive selection driving
511 or maintaining divergent gene function. For example, *hsf-1* exhibited very high polymorphism,
512 including amino acid changes at intermediate frequencies, but no instances of high impact
513 mutations likely to knock out function (Figure 6C). (We also observed poor read mapping across
514 the locus, which indicates further divergence but may also obscure deleterious mutations.) This
515 transcription factor is a master regulator of other RNAi genes, and HSF-1 activity is associated
516 with transgenerational inheritance of an on/off RNAi response (*Houri-Zeevi et al., 2020*). As *hsf-1*
517 is a potential keystone regulator of small RNA pathways, its diversification may underlie
518 significant functional variation in RNAi.

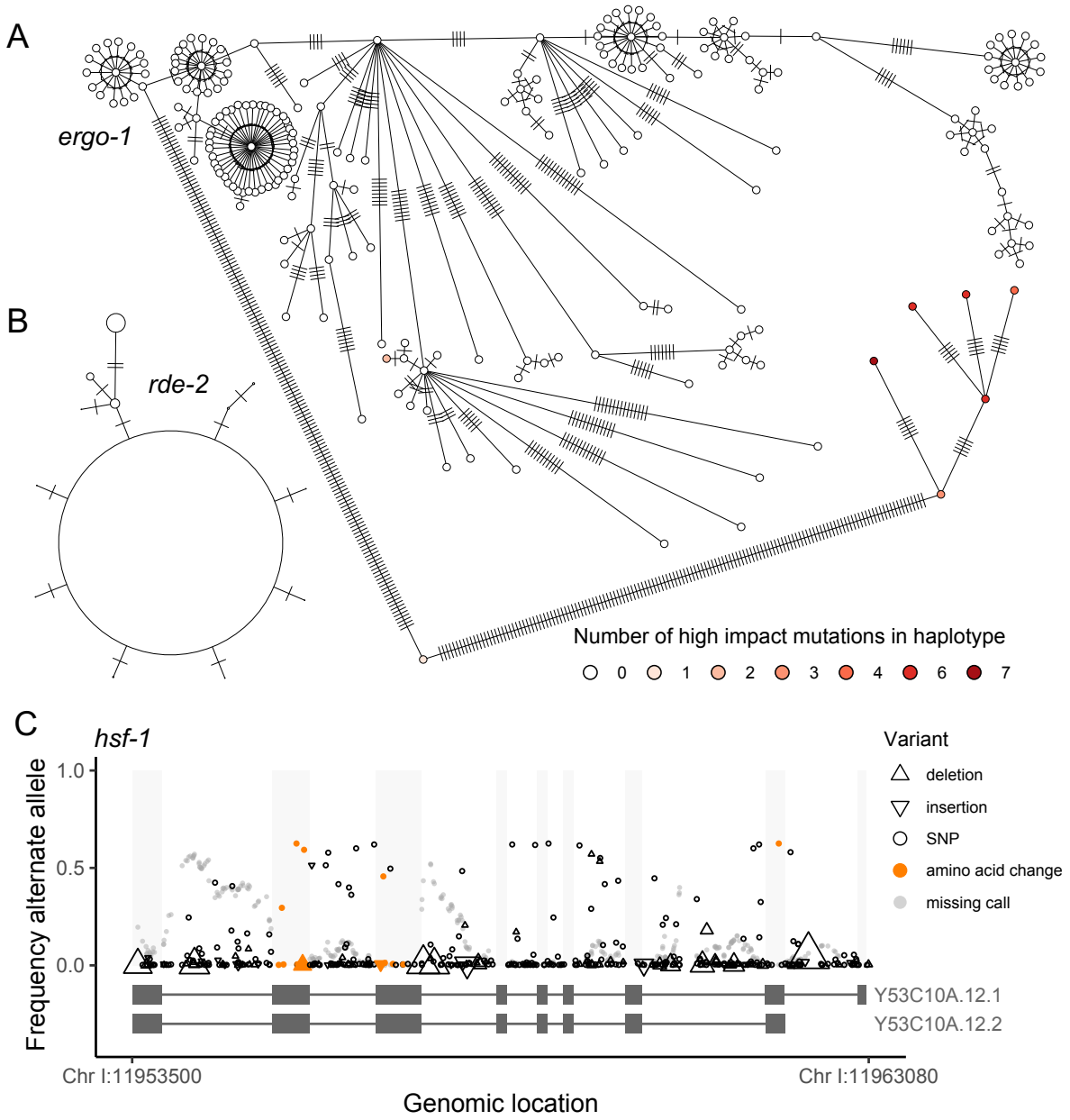

Figure 6. Population-level allelic diversity in RNAi genes across 403 strains. (A) The Argonaute *ergo-1* exhibits elevated polymorphism. Accumulation of high impact mutations in some alleles indicates gene loss by pseudogenization and implies relaxed selection. In this haplotype network, each circle represents a unique haplotype (of one or more strains) and hatch marks indicate mutations. (B) In contrast, *rde-2* exhibits conservation. Most strains belong to the common haplotype; haplotype circles are scaled by frequency. (C) The transcription factor *hsf-1* also shows elevated polymorphism. Multiple changes to the amino acid sequence, mutations segregating at intermediate frequency, and no observed high impact mutations that disrupt the protein suggest functional divergence. Each observed mutation is represented as a single point; the up- and down-triangles representing indels are scaled by indel length (range = 1-99, mean = 6.8).

530 The patterns of elevated polymorphism indicate that RNAi genes are evolving dynamically
531 within *C. elegans*, with lineage-specific trajectories of relaxed selection and gene loss, as well as
532 possible directional selection and functional divergence. These findings are consistent with our
533 experimental observations that the genetic basis of RNAi failure is strain-specific. Moreover,
534 they suggest that functional characterizations of these genes, which have been universally
535 achieved in N2, may be strain-specific as well.
536
537 **DISCUSSION**
538
539 In this study, we demonstrate that a diversity of genetic mechanisms underpins the failure of
540 some wild-type *C. elegans* strains to mount a robust germline RNAi response. Rather than
541 identifying one or more common, shared factors that explain RNAi incompetence, our results
542 indicate that RNAi fails for different reasons in different strains and that the same genes can
543 produce opposite responses. Coupled with high levels of divergence and lineage-specific
544 pseudogenization at known RNAi genes, these findings indicate that the small RNA pathways in
545 *C. elegans* are evolving rapidly and dynamically, leading to functional diversification of RNAi
546 activity.
547
548 We propose that such diversification evolved as a consequence of (a) redundancy and
549 interchangeability among Argonautes (*Billi et al., 2014; Yigit et al., 2006*), (b) competition between
550 overlapping pathways (*Yigit et al., 2006; Youngman & Claycomb, 2014*), and (c) a population
551 structure with reduced gene flow (*Dolgin et al., 2007*). Small RNA processes dominate the
552 biology of *C. elegans* (*Houri-Zeevi et al., 2020; Youngman & Claycomb, 2014*), and defenses against
553 pathogens and transposable elements may be especially susceptible to strong selection (*Nuez &*
554 *Félix, 2012*). However, because the species is globally dispersed and reproduces primarily by
555 selfing, *C. elegans* lineages evolve semi-independently, may be exposed to distinct selection
556 pressures, and may accumulate co-adapted allelic combinations (*Campbell et al., 2018; Dolgin et*
557 *al., 2007*). Argonautes and other factors are shared among pathways, and competition between
558 exogenous and endogenous RNAi can force induction of one pathway over another (*Yigit et al.,*
559 *2006; Youngman & Claycomb, 2014*). In this vein, we might imagine, for example, how selection
560 on germline maintenance in one genetic background could compromise a response to

561 environmental triggers, as well as how Argonaute redundancy could facilitate evolutionary
562 lability and gene-specific, lineage-specific responses even under similar selection pressures.
563
564 An example of competition between overlapping pathways may be reflected in some of our
565 results, as simultaneous exogenous and endogenous demands on shared factors may explain the
566 behavior of QX1211. In addition to the on/off responses among individuals (Figure 1, Figure 2),
567 QX1211 exhibits increased sensitivity to germline RNAi after consecutive generations at ≥18°C
568 (unpublished data)—but this co-occurs with onset of the mortal germline phenotype and
569 reproductive extinction, which is associated with shifts in piRNA-like pools of small RNAs
570 (*Frézal et al., 2018*). Thus, changes in RNAi activity appear to be either a cause or a consequence
571 of germline mortality in QX1211 within individual animals, which in turn may explain the
572 differences in sensitivity to exogenous RNAi. Competition between pathways may also explain
573 the *ppw-1*-dependent suppression of RNAi in QX1211 (Figure 3). If *ppw-1* is a limiting factor in
574 the defense against germline mortality in QX1211, then decreasing its availability might
575 downregulate germline protection while simultaneously releasing resources for the competing
576 exogenous pathway. QX1211 exhibited highest expression of *ppw-1* and *sago-2* (Figure 5) and
577 carries a *ppw-1*-like allele of *sago-2* (File S3)—in the most speculative case, this might reflect a
578 history of selection for *increased* germline-associated RNAi response in QX1211, even as
579 laboratory assays for exogenous RNAi reveal apparent incompetence.
580
581 Consequently, although incompetence for laboratory-induced RNAi is the explicit focus of this
582 study, we emphasize that the synthetic phenomenon of RNAi by feeding does not necessarily
583 represent processes most relevant in nature. The role of RNAi in the wild remains largely
584 obscured, though some observations offer clues. Exogenous RNAi likely induces responses that
585 evolved for antiviral immunity, as viruses that infect *C. elegans* and other *Caenorhabditis*
586 species have been discovered, notably in isolates with defective RNAi, and antiviral immunity
587 shows a clear association with an active RNAi response (*Félix et al., 2011; Sarkies et al., 2013;*
588 *Schott et al., 2005; Wilkins et al., 2005; Yigit et al., 2006*). The overlap between experimental RNAi
589 and antiviral response is incomplete, however, as variation in RNAi sensitivity does not
590 completely correlate with immunity and the systemic and transgenerational properties of RNAi
591 are not observed in viral infection (*Ashe et al., 2013, 2015; Félix et al., 2011*). Orsay virus, the only
592 naturally-occurring virus known to infect *C. elegans*, invades intestinal cells and is horizontally,

593 but not vertically, transmitted (*Félix et al., 2011; Franz et al., 2014*), though vertically transmissible
594 viral-like RNAs have been detected in the germlines of wild-caught *Caenorhabditis* isolates
595 (*Richaud et al., 2019*), suggesting undiscovered host-pathogen dynamics. Endogenous RNAi is
596 likely required for germline maintenance in the wild, as suggested by the observations in
597 QX1211. Hence the piRNA pathway, which is active in the germline and presumed critical for
598 maintaining genome integrity (*Wilson & Doudna, 2013; Youngman & Claycomb, 2014*), may
599 dominate the biology of, or be upregulated more often in, some strains relative to others (*Frézal*
600 *et al., 2018*). One possibility is that *ergo-1* gatekeeps RNAi pathway activity differently in
601 different isolates, as *ergo-1* N2 mutants show enhanced exo-RNAi but reduced endo-RNAi (*Yigit*
602 *et al., 2006*) and the *ergo-1* locus exhibits extreme allelic diversification in nature (Table 1,
603 Figure 6). Another possibility is that in the wild, RNAi in the germline matters most to future
604 generations. Strains resistant to RNAi upon exposure can show transgenerational sensitivity
605 (*Tijsterman et al., 2002*), and a growing body of research emphasizes the outsized role of RNAi in
606 transgenerational inheritance (*Houri-Zeevi et al., 2020, 2021*). Thus, RNAi as we have studied it in
607 the lab provides an oblique view into its role in nature.
608
609 Given the essentiality of RNAi to numerous biological processes—and the centrality of *C.*
610 *elegans* in RNAi research—is the variation in this system surprising? Perhaps not: even as RNAi
611 genes are shared deeply within the eukaryotic lineage (*Shabalina & Koonin, 2008; Wynant et al.,*
612 *2017*), the variation we describe here mirrors patterns of RNAi incompetence and molecular
613 evolution over longer timescales. The ability to silence genes by dsRNA appears intermittently,
614 and shows evidence of rapid evolution within the *Caenorhabditis* genus (*Nuez & Félix, 2012;*
615 *Winston et al., 2007*), across nematodes generally (*Buck & Blaxter, 2013; Dalzell et al., 2011*), and in
616 other systems (*Obbard et al., 2009*). Argonautes and associated RNAi factors also exhibit taxon-
617 specific patterns of gene duplication, loss, and diversification, likely representative of
618 diversification of biological functions (*Buck & Blaxter, 2013; Dalzell et al., 2011; Obbard et al.,*
619 *2009*). In other words, the contemporaneous variation in RNAi observed within extant *C. elegans*
620 mirrors the great lability in RNAi observed over long timescales (*Nuez & Félix, 2012*).
621
622 *C. elegans* increasingly appears to be dominated by transgenerationally inherited small RNA
623 programs (*Houri-Zeevi et al., 2020, 2021*) that vary significantly in nature (*Frézal et al., 2018*). This
624 variation offers leverage: characterization of wild-type variation can elucidate condition-

625 dependent mechanisms (*Chandler et al., 2013*), which are rampant in RNAi, a complex and
626 intricate collection of interactions susceptible to unexpected outcomes (*De-Souza et al., 2019*) and
627 sensitive to environmental conditions (*Houri-Zeevi et al., 2021*). Identifying mechanisms of
628 variation will help to bridge the gulf between our understanding of the genetics of RNAi and the
629 role of RNAi in nature, and future work may benefit from evaluating wild-type isolates in the
630 context of carefully chosen environmental perturbations (*Rockman, 2008*). For example,
631 temperature likely matters for RNAi, given the exquisite sensitivity of *C. elegans* to temperature
632 (*Testa et al., 2020*) and the intimate relationship between temperature and other stresses and RNAi
633 (*Frézal et al., 2018; Houri-Zeevi et al., 2021; Pagliuso et al., 2021*); our observations of QX1211
634 would have been obscured without rigorous temperature control. Sydney Brenner's selection of
635 *C. elegans* as a model species, and N2 as the strain of study, was fortuitous for the future
636 discovery of RNAi (*Félix, 2008*), and it remains the most fertile area for elucidating gene
637 regulation by small RNAs (*Youngman & Claycomb, 2014*). Now, characterizations of significant
638 natural genetic and functional variation in RNAi provide a new access point for expanding our
639 understanding in a system already so well established.
640

641 **MATERIALS AND METHODS**

642

643 **Strains used in this study**

644

645 Table S4 contains a complete list of strains used in this study. To introduce germline-expressed
646 GFP into wild isolates, we introgressed *zuIs178 [his-72(1kb 5' UTR)::his-*
647 *72::SRPVAT::GFP::his-72 (1KB 3' UTR) + 5.7 kb XbaI - HindIII unc-119(+)]; stIs10024 [pie-*
648 *1::H2B::GFP::pie-1 3' UTR + unc-119(+)]* into strains CB4856, ECA369, JU1522 and QX1211
649 by crossing to RW10029 and backcrossing to the wild strain for 10-18 generations.
650

651 **Worm husbandry**

652

653 Worms were cultured following standard protocol (*Stiernagle, 2006*), though we added 1.25%
654 agarose to plates used to maintain non-N2 wild isolates, to avoid burrowing. Worms were
655 maintained at 20°C without starving for at least three generations before initiating an experiment,

656 with the exception of QX1211, which was maintained at 18°C to avoid induction of the mortal
657 germline phenotype (*Frézal et al., 2018*).
658
659 **RNA interference**
660
661 *General culture conditions*
662
663 RNAi was induced by feeding and experiments were carried out on plates, at 20°C, based on
664 methods previously described (*Ahringer, 2006; Kamath et al., 2001*). In brief: to target endogenous
665 germline-expressed genes, we fed worms HT115 *E. coli* bacteria that had been transformed with
666 the pL4440-derived *par-1* (H39E23.1), *par-4* (Y59A8B.14), *pos-1* (F52E1.1), or GFP feeding
667 vector (*Timmons et al., 2001*). The *par-1* and *pos-1* vectors were obtained from the Ahringer
668 feeding library (*Kamath & Ahringer, 2003*); *par-4* was a gift from M. Mana. To target GFP, we
669 transformed HT115 with pL4417, which carries 0.7 kb of GFP coding sequence (*Timmons et al.,*
670 *2001*). We used *E. coli* carrying the empty pL4440 vector as a negative control. Bacteria were
671 streaked from frozen stocks onto LB agar plates with carbenicillin (25 ug/mL) and tetracycline
672 (12.5 mg/mL); liquid cultures were inoculated with 5-10 colonies from <1 week old plates, into
673 LB broth with carbenicillin (50 ug/mL) and tetracycline (12.5 mg/mL) and incubated for 16-
674 18hrs shaking at 37°C, then amplified in a 1:200 dilution with carbenicillin (50 ug/mL) for 6hrs.
675 Seeded plates were incubated in the dark at room temperature and used no earlier than 44hrs and
676 no later than 78hrs. Experimental worms were exposed to RNAi bacteria as L1s by hatching on
677 RNAi plates, synchronized either by bleaching (*Stiernagle, 2006*) or by timed egg-laying by the
678 hermaphrodite mothers.
679
680 *Embryonic lethality assays*
681
682 To measure RNAi response by phenotypic penetrance, we targeted *par-1* or *pos-1* transcripts in
683 the hermaphrodite germline and measured embryonic lethality in the next generation.
684 Experimental worms were reared on RNAi plates and transferred as L4s to fresh RNAi plates for
685 the egg-laying assay, remaining continuously exposed to RNAi bacteria since their hatching. For
686 all experiments except those explicitly testing variation in penetrance between individual worms
687 (Figure 1B, Figure 3C), the L4 hermaphrodites were pooled in small groups of 4-6 on 6-10

688 replicate assay plates. For the complementation tests (Figure 3, Figure 4, Figure S2), all embryos
689 within the first ~15hrs of egg-laying were scored for hatching, typically 100-200 embryos per
690 plate. For assays testing RNAi within a defined window of reproductive maturity, we scored the
691 embryos laid in a 4-6hr window within the first 8hrs of egg-laying (Figure 1A), or a 2hr window
692 4hrs after egg-laying began (Figure 2C). For the experiment measuring RNAi in individual
693 worms over their reproductive lifespan (Figure 1B, Figure S1), the L4 hermaphrodites were
694 singled to RNAi plates, permitted to lay embryos, and continually transferred to fresh plates until
695 they ceased to lay, or laid only unfertilized eggs. To score embryos as dead or alive, we removed
696 the egg-laying adult(s), incubated the plates at 20°C for 24hrs, and counted (dead) embryos and
697 hatched larvae using a stereoscope. Experiments included 6-10 (RNAi treatment) or 4-6
698 (negative control) replicate plates.
699
700 To test the effect of genotype on embryonic lethality following exposure to RNAi, the counts of
701 dead embryos and hatched larvae from each replicate plate were bound together as a single
702 response variable and modeled with a generalized linear model with a quasibinomial error
703 structure, implemented by the *glm* function in R. The model included a single linear predictor for
704 genotype and took the form $E(Y)=g^{-1}(\beta_0+\beta_{genotype})$. Within each experiment, differences between
705 specific genotypes were assessed by pairwise contrasts using the "Tukey" specification in the
706 function *glht* in the R package *multcomp* (*Hothorn et al., 2008*).
707
708 *RNAi against GFP*
709
710 To measure germline RNAi by GFP knockdown, worms carrying a histone-linked GFP driven by
711 a *pie-1* promoter were fed RNAi bacteria targeting GFP. Synchronized animals were grown on
712 RNAi plates, then individually selected for imaging at the following stages: young adults (6±2hrs
713 after exiting L4 stage), day one adults (24±2hrs), and day 2 adults (48±2hrs). For whole worm
714 fluorescence imaging, animals were anesthetized with 10mM NaN_3 and mounted on 2% agarose
715 pads, then imaged using a 10× objective with the PerkinElmer UltraVIEW VoX spinning disk
716 confocal microscope equipped with an EM-CCD camera. Raw images were exported as
717 OME.TIFF files. We used Fiji (*Schindelin et al., 2012*) to acquire the sums of intensity in the Z
718 projection, then quantitated the GFP fluorescence by subtracting the integrated intensity of the
719 background, over the area of the worm, from the integrated intensity of the whole animal. To test

720 whether RNAi-treated worms exhibited reduced fluorescence relative to control worms, we
721 analyzed the six samples (three treatment timepoints, three control timepoints) for each strain
722 using a one-way ANOVA, then performed treatment-control contrasts within each timepoint
723 using the R function *TukeyHSD()*.
724
725 **Single-molecule fluorescence *in situ* hybridization**
726
727 *Sample preparation and imaging*
728
729 Custom Stellaris FISH probes were designed with the Stellaris Probe Designer (LGC Biosearch
730 Technologies). We excluded polymorphic sites during probe design. Worms were synchronized
731 on tryptone-free NGM agar plates at the L1 stage and reared on RNAi bacteria as described
732 above. Embryos were extracted by standard bleaching/washing, fixed using 3.7% formaldehyde
733 in RNase-free phosphate buffered saline, and hybridized (100nM at 37°C for 4hrs) with a Quasar
734 570 labeled probe set targeting either *par-1* or *par-4*, following the manufacturer's instructions.
735 Samples were mounted using VECTASHIELD antifade mounting medium with DAPI (Vector
736 Labs #H-1200) on no. 1 cover slides. Images were captured with a 100X oil immersion objective
737 on a PerkinElmer UltraVIEW VoX spinning disk confocal microscope equipped with an EM-
738 CCD camera and piezoelectric motorized stage. Three-dimensional image stacks were collected
739 using Volocity 3D visualization software (PerkinElmer) and exported as TIFF files.
740
741 *Quantitative Analysis*
742
743 Image segmentation masks were applied and chromosome clusters were counted using ImageJ
744 (*Schneider et al., 2012*). Quantification of single molecule FISH spots was performed using Aro, a
745 MATLAB-based, machine learning pipeline designed for single-molecule visualization in worm
746 embryos (*Wu & Rifkin, 2015*). The training sets for the random forest classifier were generated
747 from multiple samples of each genetic background and treatment. To test whether means or
748 variances in transcript counts differed for RNAi-treated versus untreated samples within a strain,
749 we applied two-sample *t*-tests and *F*-tests, respectively. For these tests, we only considered early
750 stage embryos (up to four cells). To evaluate changes in transcript abundance over a wider range
751 of embryonic development, we considered embryos with up to 30 nuclei and used ANCOVA to

752 ask whether, adjusted for embryo stage, transcript levels varied across strains within the negative
753 control condition; and whether, adjusted for embryo stage, transcript levels varied between
754 control and treatment conditions within a strain. We used minimal model selection to test for
755 changes in the way transcript level depended upon embryo stage (i.e. changes in slope). We
756 estimated ANCOVA effect sizes as ω^2 using the R package *sjstats* (*Lüdecke, 2018*).
757
758 **RNA-seq**
759
760 *Library preparation and sequencing*
761
762 Healthy cultures of strains N2, CB4856, QX1211, JU1088 and EG4348, reared for several
763 generations without starving or bleaching, were bleached to retrieve large numbers of embryos.
764 Synchronized L1 larvae were reared on plates with the empty RNAi feeding vector, details as
765 described above. Young, reproductively mature hermaphrodites were washed off plates and
766 rinsed twice with M9, then RNA was extracted with TRIzol (Invitrogen #15596026) and RNeasy
767 columns (Qiagen #74104), following (*He, 2011*). All samples were collected and processed
768 simultaneously and in triplicate, starting with replicate plates of worms. Libraries were prepared
769 with the NEBNext Ultra II Directional RNA Library Prep Kit for Illumina (NEB #7760), with
770 cDNA generated from fresh RNA samples using 500ng of RNA and 10 cycles of PCR. Libraries
771 were quality checked using an Agilent 2100 Bioanalyzer and fragments were size-selected via
772 BluePippon (Sage Science). Libraries were sequenced on an Illumina NextSeq for single-end
773 75bp reads at the Molecular Evolution Core facility at the Georgia Institute of Technology.
774
775 *Alignment and gene expression quantification*
776
777 We generated strain-specific transcriptomes for RNA-seq read quantification by patching SNPs
778 and INDELs from CeNDR (release 20210121) (*Cook et al., 2017*) onto the N2 reference genome
779 (release ws276) (*Harris et al., 2020*) using *g2gtools* (v0.1.31 via conda v4.7.12, Python v2.7.16)
780 (https://github.com/churchill-lab/g2gtools), followed by transcriptome extraction. Specifically,
781 for each non-reference strain, INDELs were first chained onto the reference genome using
782 *g2gtools vcf2chain* and SNPs were patched onto the reference genome FASTA using *g2gtools*
783 *patch*. Next, INDELs were chained onto the SNP-patched genome using *g2gtools transform* and

strain-specific GTFs were created from this updated genome FASTA via *g2gtools convert*. Strain-specific transcriptomes were generated from these strain-specific genome FASTAs and GTFs using *gffread* (v0.12.7) (*Pertea & Pertea, 2020*).

Transcript-level quantification was performed using Salmon (v1.4.0) (*Patro et al., 2017*). Before Salmon quantification, Illumina TruSeq adapters were trimmed from RNA-seq reads using Trimmomatic (v0.3.9) (*Bolger et al., 2014*) with parameters *ILLUMINACLIP:TruSeq3-SE.fa:1:30:12*. Salmon index files were built from the strain-specific transcriptomes using command *salmon index* with options *-k 31 --keepDuplicates* (all others default; no decoy was used). Transcript quantification was performed with *salmon quant* with options *-l SR --dumpEq, --rangeFactorizationBins 4, --seqBias, and --gcBias*, and the library-specific fragment length arguments *--fldMean* and *--fldSD*.

Analysis of gene expression

We performed all expression analyses in R (v4.0.3) (*R Core Team, 2020*) using data processed with the DESeq2 package (v1.32.0) (*Love et al., 2014*). We used the *tximport* package (v1.20.0) (*Soneson et al., 2015*) to import Salmon transcript quantification data into DESeq2 and to compute gene-level expression quantification estimates. Genes with 10 or fewer counts total across all samples after *tximport* were excluded from downstream analysis (18,589 genes retained).

To test for differential expression across strains, gene counts were modeled using the negative binomial generalized linear model in DESeq2:

$$\log2(q_{ij}) = \beta_i \, x_j \, ,$$

where for gene i, sample j, q is proportional to the true concentration of RNA fragments for the gene. β_i gives the log2 fold changes for gene i and x represents the strain; batch was not included in the model because all samples (three biological replicates per strain, five strains) were processed simultaneously. Significance testing for differential expression was performed by likelihood ratio test (LRT) in DESeq2, which captured strain-wise significance by comparing the above model to a reduced model containing only the intercept (*Love et al., 2014*). Genes were considered differentially expressed by strain if the genome-wide adjusted p-value (FDR) from the LRT was <0.1 (5,464 of the 18,589 genes passed this threshold overall). Estimates of

816 differential expression between N2 and each other strain were extracted via pairwise contrasts;
817 effect sizes and p-values were corrected using the '*ashr'* method from the *ashr* package (v2.2-
818 47) *(Stephens, 2017*).
819
820 We assessed strain-wise variance per gene by first obtaining normalized gene expression data
821 from the variance-stabilizing transformation (*vst* function) in DESeq2. This transformation puts
822 the data in log2 scale, incorporates library size and gene length normalizations, and makes the
823 variance independent of the mean (*Love et al., 2014*). Strain-wise variance for each gene was then
824 estimated by one-way ANOVA, i.e. *counts ~ strain*; the sums of squares for the strain term was
825 extracted using the *aov* function.
826
827 Expression-matched gene sets for the RNAi genes were constructed by first identifying, for each
828 RNAi gene, all genes with *vst*-normalized mean expression (across all samples) within one
829 percentile of the RNAi gene's mean expression (+/- 0.005 in expression quartile). One of these
830 genes was chosen at random for each RNAi gene, and this procedure was repeated 10,000 times
831 to obtain the 10,000 random expression-matched gene sets. The median strain-wise variance (of
832 *vst*-normalized gene counts) for each random set of genes was computed and compared to the
833 median strain-wise variance of the RNAi genes.
834
835 **Droplet digital PCR**
836
837 To design an unbiased primer set, we identified regions of identical sequence between *ppw-1* and
838 *sago-2* and across the ten strains of interest. Following (*Kamitaki et al., 2018*), we chose primers
839 to target both genes, and probes to discriminate between *ppw-1* (FAM) and *sago-2* (HEX).
840 Sequences are as follows: forward (CTTGGTACCGCTCCGCTC), reverse
841 (GCTGATTCGGTTTGATCGTC), *ppw-1* probe (AGACGAGAAATGTGGAGAGGGGAA),
842 *sago-2* probe (AGACGAGAAATGAGGAGTGGGGAA). Both probes anneal in the same
843 location, ensuring competition between them.
844
845 Worms from strains N2, CB4856, CB4852, DL238, ECA369, EG4348, JU1088, JU1581,
846 KR314, and QX1211 were reared under standard conditions (as above), bleached to isolate
847 embryos, and grown to reproductive maturity. RNA was extracted with TRIzol (Invitrogen

848 #15596026) and RNeasy columns (Qiagen #74104), following (*He, 2011*). RNA was collected at
849 two timepoints, early and middle reproductive maturity (68±2hrs and 90±2hrs after bleaching,
850 respectively). RNA sample concentrations were quantified and standardized using a Nanodrop
851 (Thermo Scientific), and cDNA was synthesized using the ProtoScript II First Stand cDNA
852 Synthesis Kit (NEB #E6560S). The experiment was replicated as follows: from each
853 experimental condition, we collected two RNA samples, for two biological replicates; within the
854 plate, each reaction was duplicated, for two technical replicates; and we conducted the entire
855 experiment twice.
856
857 Droplet digital PCR was carried out with the Bio-Rad QX200 system following the
858 manufacturer's protocol, and results were obtained using the QuantaSoft software (Bio-Rad), via
859 automatic thresholding followed by manual confirmation of droplet selection. All samples
860 produced >8000 droplets and results from all samples were retained. Concentration, given by
861 number of copies per μL, was modeled with a quasipoisson error structure using the *glm()*
862 function in R. As *ppw-1* was detected at an order of magnitude higher than *sago-2*, we analyzed
863 the two genes separately. By model selection, we identified the minimal model that best
864 described the observed differences in concentration For the *ppw-1* analysis, we dropped run date
865 from the model, as it was not significant; for *sago-2*, run date contributed <1% to the total
866 observed deviance (Table S2), but was nevertheless significant, so it was retained. The final
867 models were: Concentration ~ Strain*DevStage/BiolRep for *ppw-1*, and Concentration ~
868 RunDate + Strain*DevStage/BiolRep for *sago-2*. To determine which strains differed in *ppw-1*
869 or *sago-2* levels, we performed pairwise contrasts among strains using the *TukeyHSD()* function
870 and a family-wise confidence level of 95% (only a subset of comparisons are reported in the
871 text). To determine which strains showed differences in concentration according to
872 developmental stage, we performed pairwise contrasts using the *lsmeans()* function in the
873 package *lsmeans*, using a confidence level of 95% following a Bonferroni correction for multiple
874 tests.
875
876 **Genotype and sequence analysis**
877
878 To evaluate population-level allelic variation at known RNAi genes, we queried the *C. elegans*
879 Natural Diversity Resource (https://elegansvariation.org), which provides genotype data for 403

880 wild isotypes from short read sequence data mapped to the N2 reference genome (*Cook et al.,*
881 *2017*). Specifically, we downloaded the VCF (WI.20200815.hard-filter.isotype.vcf) and used the
882 R package *VariantAnnotation* (*Obenchain et al., 2014*) to extract information about mutations and
883 mapping coverage, and the package *PopGenome* (*Pfeifer et al., 2014*) to estimate nucleotide
884 diversity, at each gene. Haplotype networks for individual genes were determined using the R
885 package *pegas* (*Paradis, 2010*).
886
887 For a subset of strains, we verified and/or supplemented the genotype data with de novo-
888 assembled genome data and long read data. Genomic DNA of strains AB2, EG4347, EG4348,
889 JU1088, JU1171, PB306, PX174, QX1211 and QX1216 was prepared using standard
890 phenol/chloroform extraction and ethanol precipitation. Samples were cleaned with DNA Clean
891 & Concentrator columns (Zymo Research #D4004) and libraries were prepared using NEBNext
892 Ultra II FS DNA Library Prep Kit for Illumina (New England Biolabs #E7805) and Multiplex
893 Oligos for Illumina (NEB #E7500), with customized fragmentation and purification steps to
894 enrich for desired sizes. A final DNA size selection targeting 650bp±50bp was performed using
895 BluePippin (Sage Science). The libraries were sequenced on a HiSeq 2500 (Illumina) on Rapid
896 Run Mode (paired-end 2x250bp) in the Molecular Evolution Core at the Georgia Institute of
897 Technology. Raw data were trimmed using Cutadapt (v1.18) (*Martin, 2011*) and quality control
898 was performed with FastQC (*Andrews, 2021*). Reads were then assembled into contigs with
899 DISCOVAR *de novo* (v52488) (Broad Institute) using default parameters. Separately, QX1211
900 and JU1088 genomic DNA samples were snap frozen with liquid nitrogen and sent to the
901 Georgia Genomics and Bioinformatics Core (GGBC) at the University of Georgia. Quality was
902 assessed by Qubit (Invitrogen) and NanoDrop (Thermo Scientific), molecular weight distribution
903 was assessed by fragment analysis, and sizes >15kb were selected by BluePippin (Sage Science).
904 Each sample was sequenced on a single SMRT Cell on the PacBio Sequel I platform (Pacific
905 Biosciences). Genome assembly was performed by the GGBC using Canu (v1.7) (*Koren et al.,*
906 *2017*).
907
908 **Computing**
909
910 Unless otherwise specified, all analyses were performed in R (*R Core Team, 2021*) and figures
911 were generated with the packages *ggplot2* (*Wickham, 2016*) and *ggpubr* (*Kassambara, 2020*).

Computationally intensive jobs, including read mapping and genome assembly, were performed on PACE, the high performance computing platform at the Georgia Institute of Technology.

ACKNOWLEDGEMENTS

We wish to acknowledge the core facilities at the Parker H. Petit Institute for Bioengineering and Bioscience at the Georgia Institute of Technology for the use of their shared equipment, services and expertise. Specifically, we are grateful to Aaron Lifland at the Optimal Microscopy Core for training in confocal imaging, and Anton Bryksin, Naima Djeddar, and Shweta Biliya at the Molecular Evolution Core for collaboration on the sequencing projects. We also thank the Georgia Genomics and Bioinformatics Core at the University of Georgia for PacBio sequencing and genome assembly. We thank Miyeko Mana for the gift of the *par-4* RNAi clone, and Lijiang Long and Patrick McGrath for strain PTM377. Some strains were provided by the CGC, which is funded by NIH Office of Research Infrastructure Programs (P40 OD010440). This research was supported in part through research cyberinfrastructure resources and services provided by the Partnership for an Advanced Computing Environment (PACE) at the Georgia Institute of Technology. This research was funded by NIH grant R35 GM119744 to A.B.P, NSF grant MCB1518314 to D.A.P., and NSF fellowship 2109666 to A.D.B.

LITERATURE CITED

Ahringer, J. (2006). Reverse genetics. In *WormBook: The Online Review of C. elegans Biology [Internet]*. WormBook. https://www.ncbi.nlm.nih.gov/books/NBK19711/

Andersen, E. C., Gerke, J. P., Shapiro, J. A., Crissman, J. R., Ghosh, R., Bloom, J. S., Félix, M.-A., & Kruglyak, L. (2012). Chromosome-scale selective sweeps shape Caenorhabditis elegans genomic diversity. *Nature Genetics*, *44*(3), 285–290. https://doi.org/10.1038/ng.1050

Andrews, S. (2021). *FastQC: A quality control tool for high throughput sequence data*. https://www.bioinformatics.babraham.ac.uk/projects/fastqc/

Ashe, A., Bélicard, T., Le Pen, J., Sarkies, P., Frézal, L., Lehrbach, N. J., Félix, M.-A., & Miska, E. A. (2013). A deletion polymorphism in the Caenorhabditis elegans RIG-I homolog disables viral RNA dicing and antiviral immunity. *ELife*, *2*, e00994. https://doi.org/10.7554/eLife.00994

Ashe, A., Sarkies, P., Le Pen, J., Tanguy, M., & Miska, E. A. (2015). Antiviral RNA Interference against Orsay Virus Is neither Systemic nor Transgenerational in Caenorhabditis elegans. *Journal of Virology*, *89*(23), 12035–12046. https://doi.org/10.1128/JVI.03664-14

Ben-David, E., Burga, A., & Kruglyak, L. (2017). A maternal-effect selfish genetic element in Caenorhabditis elegans. *Science (New York, N.Y.)*, *356*(6342), 1051–1055. https://doi.org/10.1126/science.aan0621

Billi, A. C., Fischer, S. E. J., & Kim, J. K. (2014). Endogenous RNAi pathways in C. elegans. *WormBook: The Online Review of C. Elegans Biology*, 1–49. https://doi.org/10.1895/wormbook.1.170.1

Bolger, A. M., Lohse, M., & Usadel, B. (2014). Trimmomatic: A flexible trimmer for Illumina sequence data. *Bioinformatics (Oxford, England)*, *30*(15), 2114–2120. https://doi.org/10.1093/bioinformatics/btu170

Buck, A. H., & Blaxter, M. (2013). Functional diversification of Argonautes in nematodes: An expanding universe. *Biochemical Society Transactions*, *41*(4), 881–886. https://doi.org/10.1042/BST20130086

Campbell, R. F., McGrath, P. T., & Paaby, A. B. (2018). Analysis of Epistasis in Natural Traits Using Model Organisms. *Trends in Genetics: TIG*, *34*(11), 883–898. https://doi.org/10.1016/j.tig.2018.08.002

Chandler, C. H., Chari, S., & Dworkin, I. (2013). Does your gene need a background check? How genetic background impacts the analysis of mutations, genes, and evolution. *Trends in Genetics: TIG*, *29*(6), 358–366. https://doi.org/10.1016/j.tig.2013.01.009

Charles, S., Aubry, G., Chou, H.-T., Paaby, A. B., & Lu, H. (2021). High-Temporal-Resolution smFISH Method for Gene Expression Studies in Caenorhabditis elegans Embryos. *Analytical Chemistry*, *93*(3), 1369–1376. https://doi.org/10.1021/acs.analchem.0c02966

Cook, D. E., Zdraljevic, S., Roberts, J. P., & Andersen, E. C. (2017). CeNDR, the Caenorhabditis elegans natural diversity resource. *Nucleic Acids Research*, *45*(D1), D650–D657. https://doi.org/10.1093/nar/gkw893

Crombie, T. A., Zdraljevic, S., Cook, D. E., Tanny, R. E., Brady, S. C., Wang, Y., Evans, K. S., Hahnel, S., Lee, D., Rodriguez, B. C., Zhang, G., van der Zwagg, J., Kiontke, K., & Andersen, E. C. (2019). Deep sampling of Hawaiian Caenorhabditis elegans reveals high genetic diversity and admixture with global populations. *ELife*, *8*, e50465. https://doi.org/10.7554/eLife.50465

Dalzell, J. J., McVeigh, P., Warnock, N. D., Mitreva, M., Bird, D. M., Abad, P., Fleming, C. C., Day, T. A., Mousley, A., Marks, N. J., & Maule, A. G. (2011). RNAi effector diversity in nematodes. *PLoS Neglected Tropical Diseases*, *5*(6), e1176. https://doi.org/10.1371/journal.pntd.0001176

De-Souza, E. A., Camara, H., Salgueiro, W. G., Moro, R. P., Knittel, T. L., Tonon, G., Pinto, S., Pinca, A. P. F., Antebi, A., Pasquinelli, A. E., Massirer, K. B., & Mori, M. A. (2019). RNA interference may result in unexpected phenotypes in Caenorhabditis elegans. *Nucleic Acids Research*, *47*(8), 3957–3969. https://doi.org/10.1093/nar/gkz154

Dolgin, E. S., Charlesworth, B., Baird, S. E., & Cutter, A. D. (2007). Inbreeding and Outbreeding Depression in Caenorhabditis Nematodes. *Evolution*, *61*(6), 1339–1352. https://doi.org/10.1111/j.1558-5646.2007.00118.x

Elvin, M., Snoek, L. B., Frejno, M., Klemstein, U., Kammenga, J. E., & Poulin, G. B. (2011). A fitness assay for comparing RNAi effects across multiple C. elegans genotypes. *BMC Genomics*, *12*, 510. https://doi.org/10.1186/1471-2164-12-510

Félix, M.-A. (2008). RNA interference in nematodes and the chance that favored Sydney Brenner. *Journal of Biology*, *7*(9), 34. https://doi.org/10.1186/jbiol97

Félix, M.-A., Ashe, A., Piffaretti, J., Wu, G., Nuez, I., Bélicard, T., Jiang, Y., Zhao, G., Franz, C. J., Goldstein, L. D., Sanroman, M., Miska, E. A., & Wang, D. (2011). Natural and

995 experimental infection of Caenorhabditis nematodes by novel viruses related to
996 nodaviruses. *PLoS Biology*, *9*(1), e1000586. https://doi.org/10.1371/journal.pbio.1000586
997 Fire, A., Xu, S., Montgomery, M. K., Kostas, S. A., Driver, S. E., & Mello, C. C. (1998). Potent
998 and specific genetic interference by double-stranded RNA in Caenorhabditis elegans.
999 *Nature*, *391*(6669), 806–811. https://doi.org/10.1038/35888
1000 Franz, C. J., Renshaw, H., Frezal, L., Jiang, Y., Félix, M.-A., & Wang, D. (2014). Orsay,
1001 Santeuil and Le Blanc viruses primarily infect intestinal cells in Caenorhabditis nematodes.
1002 *Virology*, *448*, 255–264. https://doi.org/10.1016/j.virol.2013.09.024
1003 Frézal, L., Demoinet, E., Braendle, C., Miska, E., & Félix, M.-A. (2018). Natural genetic
1004 variation in a multigenerational phenotype in C. elegans. *Current Biology : CB*, *28*(16),
1005 2588-2596.e8. https://doi.org/10.1016/j.cub.2018.05.091
1006 Grishok, A. (2013). Biology and Mechanisms of Short RNAs in Caenorhabditis elegans.
1007 *Advances in Genetics*, *83*, 1–69. https://doi.org/10.1016/B978-0-12-407675-4.00001-8
1008 Harris, T. W., Arnaboldi, V., Cain, S., Chan, J., Chen, W. J., Cho, J., Davis, P., Gao, S., Grove,
1009 C. A., Kishore, R., Lee, R. Y. N., Muller, H.-M., Nakamura, C., Nuin, P., Paulini, M.,
1010 Raciti, D., Rodgers, F. H., Russell, M., Schindelman, G., … Sternberg, P. W. (2020).
1011 WormBase: A modern Model Organism Information Resource. *Nucleic Acids Research*,
1012 *48*(D1), D762–D767. https://doi.org/10.1093/nar/gkz920
1013 He, F. (2011). Total RNA Extraction from C. elegans. *Bio-Protocol*, e47–e47.
1014 Hothorn, T., Bretz, F., & Westfall, P. (2008). Simultaneous inference in general parametric
1015 models. *Biometrical Journal. Biometrische Zeitschrift*, *50*(3), 346–363.
1016 https://doi.org/10.1002/bimj.200810425
1017 Houri-Zeevi, L., Korem Kohanim, Y., Antonova, O., & Rechavi, O. (2020). Three Rules Explain
1018 Transgenerational Small RNA Inheritance in C. elegans. *Cell*, *182*(5), 1186-1197.e12.
1019 https://doi.org/10.1016/j.cell.2020.07.022
1020 Houri-Zeevi, L., Teichman, G., Gingold, H., & Rechavi, O. (2021). Stress resets ancestral
1021 heritable small RNA responses. *ELife*, *10*, e65797. https://doi.org/10.7554/eLife.65797
1022 Kamath, R. S., & Ahringer, J. (2003). Genome-wide RNAi screening in Caenorhabditis elegans.
1023 *Methods (San Diego, Calif.)*, *30*(4), 313–321. https://doi.org/10.1016/s1046-
1024 2023(03)00050-1
1025 Kamath, R. S., Fraser, A. G., Dong, Y., Poulin, G., Durbin, R., Gotta, M., Kanapin, A., Le Bot,
1026 N., Moreno, S., Sohrmann, M., Welchman, D. P., Zipperlen, P., & Ahringer, J. (2003).
1027 Systematic functional analysis of the Caenorhabditis elegans genome using RNAi. *Nature*,
1028 *421*(6920), 231–237. https://doi.org/10.1038/nature01278
1029 Kamath, R. S., Martinez-Campos, M., Zipperlen, P., Fraser, A. G., & Ahringer, J. (2001).
1030 Effectiveness of specific RNA-mediated interference through ingested double-stranded
1031 RNA in Caenorhabditis elegans. *Genome Biology*, *2*(1), RESEARCH0002.
1032 https://doi.org/10.1186/gb-2000-2-1-research0002
1033 Kamitaki, N., Usher, C. L., & McCarroll, S. A. (2018). Using Droplet Digital PCR to Analyze
1034 Allele-Specific RNA Expression. *Methods in Molecular Biology (Clifton, N.J.)*, *1768*, 401–
1035 422. https://doi.org/10.1007/978-1-4939-7778-9_23
1036 Kassambara, A. (2020). *ggpubr: "ggplot2" Based Publication Ready Plots*.
1037 https://rpkgs.datanovia.com/ggpubr/
1038 Koren, S., Walenz, B. P., Berlin, K., Miller, J. R., Bergman, N. H., & Phillippy, A. M. (2017).
1039 Canu: Scalable and accurate long-read assembly via adaptive k-mer weighting and repeat
1040 separation. *Genome Research*, *27*(5), 722–736. https://doi.org/10.1101/gr.215087.116
1041 Lee, D., Zdraljevic, S., Stevens, L., Wang, Y., Tanny, R. E., Crombie, T. A., Cook, D. E.,
1042 Webster, A. K., Chirakar, R., Baugh, L. R., Sterken, M. G., Braendle, C., Félix, M.-A.,

Rockman, M. V., & Andersen, E. C. (2021). Balancing selection maintains hyper-divergent haplotypes in Caenorhabditis elegans. *Nature Ecology & Evolution*, *5*(6), 794–807. https://doi.org/10.1038/s41559-021-01435-x

Love, M. I., Huber, W., & Anders, S. (2014). Moderated estimation of fold change and dispersion for RNA-seq data with DESeq2. *Genome Biology*, *15*(12), 550. https://doi.org/10.1186/s13059-014-0550-8

Lüdecke, D. (2018). *sjstats: Statistical Functions for Regression Models.* Zenodo. https://doi.org/10.5281/zenodo.1489175

Martin, M. (2011). Cutadapt removes adapter sequences from high-throughput sequencing reads. *EMBnet.Journal*, *17*(1), 10–12. https://doi.org/10.14806/ej.17.1.200

Nuez, I., & Félix, M.-A. (2012). Evolution of susceptibility to ingested double-stranded RNAs in Caenorhabditis nematodes. *PloS One*, *7*(1), e29811. https://doi.org/10.1371/journal.pone.0029811

Obbard, D. J., Gordon, K. H. J., Buck, A. H., & Jiggins, F. M. (2009). The evolution of RNAi as a defence against viruses and transposable elements. *Philosophical Transactions of the Royal Society B: Biological Sciences*, *364*(1513), 99–115. https://doi.org/10.1098/rstb.2008.0168

Obenchain, V., Lawrence, M., Carey, V., Gogarten, S., Shannon, P., & Morgan, M. (2014). VariantAnnotation: A Bioconductor package for exploration and annotation of genetic variants. *Bioinformatics (Oxford, England)*, *30*(14), 2076–2078. https://doi.org/10.1093/bioinformatics/btu168

Paaby, A. B., White, A. G., Riccardi, D. D., Gunsalus, K. C., Piano, F., & Rockman, M. V. (2015). Wild worm embryogenesis harbors ubiquitous polygenic modifier variation. *ELife*, *4*. https://doi.org/10.7554/eLife.09178

Pagliuso, D. C., Bodas, D. M., & Pasquinelli, A. E. (2021). Recovery from heat shock requires the microRNA pathway in Caenorhabditis elegans. *PLOS Genetics*, *17*(8), e1009734. https://doi.org/10.1371/journal.pgen.1009734

Paradis, E. (2010). pegas: An R package for population genetics with an integrated-modular approach. *Bioinformatics (Oxford, England)*, *26*(3), 419–420. https://doi.org/10.1093/bioinformatics/btp696

Patro, R., Duggal, G., Love, M. I., Irizarry, R. A., & Kingsford, C. (2017). Salmon provides fast and bias-aware quantification of transcript expression. *Nature Methods*, *14*(4), 417–419. https://doi.org/10.1038/nmeth.4197

Pertea, G., & Pertea, M. (2020). GFF Utilities: GffRead and GffCompare. *F1000Research*, *9*, ISCB Comm J-304. https://doi.org/10.12688/f1000research.23297.2

Pfeifer, B., Wittelsbürger, U., Ramos-Onsins, S. E., & Lercher, M. J. (2014). PopGenome: An efficient Swiss army knife for population genomic analyses in R. *Molecular Biology and Evolution*, *31*(7), 1929–1936. https://doi.org/10.1093/molbev/msu136

Pollard, D. A., & Rockman, M. V. (2013). Resistance to germline RNA interference in a Caenorhabditis elegans wild isolate exhibits complexity and nonadditivity. *G3 (Bethesda, Md.)*, *3*(6), 941–947. https://doi.org/10.1534/g3.113.005785

R Core Team. (2020). *R: A language and environment for statistical computing*. R Foundation for Statistical Computing. https://www.R-project.org/

Raj, A., van den Bogaard, P., Rifkin, S. A., van Oudenaarden, A., & Tyagi, S. (2008). Imaging individual mRNA molecules using multiple singly labeled probes. *Nature Methods*, *5*(10), 877–879. https://doi.org/10.1038/nmeth.1253

Richaud, A., Frézal, L., Tahan, S., Jiang, H., Blatter, J. A., Zhao, G., Kaur, T., Wang, D., & Félix, M.-A. (2019). Vertical transmission in Caenorhabditis nematodes of RNA molecules

encoding a viral RNA-dependent RNA polymerase. *Proceedings of the National Academy of Sciences of the United States of America*, *116*(49), 24738–24747. https://doi.org/10.1073/pnas.1903903116

Rockman, M. V. (2008). Reverse engineering the genotype–phenotype map with natural genetic variation. *Nature*, *456*(7223), 738–744. https://doi.org/10.1038/nature07633

Rual, J.-F., Ceron, J., Koreth, J., Hao, T., Nicot, A.-S., Hirozane-Kishikawa, T., Vandenhaute, J., Orkin, S. H., Hill, D. E., van den Heuvel, S., & Vidal, M. (2004). Toward improving Caenorhabditis elegans phenome mapping with an ORFeome-based RNAi library. *Genome Research*, *14*(10B), 2162–2168. https://doi.org/10.1101/gr.2505604

Sarkies, P., Ashe, A., Le Pen, J., McKie, M. A., & Miska, E. A. (2013). Competition between virus-derived and endogenous small RNAs regulates gene expression in Caenorhabditis elegans. *Genome Research*, *23*(8), 1258–1270. https://doi.org/10.1101/gr.153296.112

Schindelin, J., Arganda-Carreras, I., Frise, E., Kaynig, V., Longair, M., Pietzsch, T., Preibisch, S., Rueden, C., Saalfeld, S., Schmid, B., Tinevez, J.-Y., White, D. J., Hartenstein, V., Eliceiri, K., Tomancak, P., & Cardona, A. (2012). Fiji: An open-source platform for biological-image analysis. *Nature Methods*, *9*(7), 676–682. https://doi.org/10.1038/nmeth.2019

Schneider, C. A., Rasband, W. S., & Eliceiri, K. W. (2012). NIH Image to ImageJ: 25 years of image analysis. *Nature Methods*, *9*(7), 671–675. https://doi.org/10.1038/nmeth.2089

Schott, D. H., Cureton, D. K., Whelan, S. P., & Hunter, C. P. (2005). An antiviral role for the RNA interference machinery in Caenorhabditis elegans. *Proceedings of the National Academy of Sciences of the United States of America*, *102*(51), 18420–18424. https://doi.org/10.1073/pnas.0507123102

Seidel, H. S., Ailion, M., Li, J., van Oudenaarden, A., Rockman, M. V., & Kruglyak, L. (2011). A novel sperm-delivered toxin causes late-stage embryo lethality and transmission ratio distortion in C. elegans. *PLoS Biology*, *9*(7), e1001115. https://doi.org/10.1371/journal.pbio.1001115

Seidel, H. S., Rockman, M. V., & Kruglyak, L. (2008). Widespread genetic incompatibility in C. elegans maintained by balancing selection. *Science (New York, N.Y.)*, *319*(5863), 589–594. https://doi.org/10.1126/science.1151107

Shabalina, S. A., & Koonin, E. V. (2008). Origins and evolution of eukaryotic RNA interference. *Trends in Ecology & Evolution*, *23*(10), 578–587. https://doi.org/10.1016/j.tree.2008.06.005

Soneson, C., Love, M. I., & Robinson, M. D. (2015). Differential analyses for RNA-seq: Transcript-level estimates improve gene-level inferences. *F1000Research*, *4*, 1521. https://doi.org/10.12688/f1000research.7563.2

Stephens, M. (2017). False discovery rates: A new deal. *Biostatistics (Oxford, England)*, *18*(2), 275–294. https://doi.org/10.1093/biostatistics/kxw041

Stiernagle, T. (2006). Maintenance of C. elegans. *WormBook: The Online Review of C. Elegans Biology*, 1–11. https://doi.org/10.1895/wormbook.1.101.1

Testa, N. D., Kaul, S., Le, K. N., Zhan, M., Lu, H., & Paaby, A. B. (2020). A portable, low-cost device for precise control of specimen temperature under stereomicroscopes. *PloS One*, *15*(3), e0230241. https://doi.org/10.1371/journal.pone.0230241

Tijsterman, M., Okihara, K. L., Thijssen, K., & Plasterk, R. H. A. (2002). PPW-1, a PAZ/PIWI protein required for efficient germline RNAi, is defective in a natural isolate of C. elegans. *Current Biology: CB*, *12*(17), 1535–1540. https://doi.org/10.1016/s0960-9822(02)01110-7

Timmons, L., Court, D. L., & Fire, A. (2001). Ingestion of bacterially expressed dsRNAs can produce specific and potent genetic interference in Caenorhabditis elegans. *Gene*, *263*(1–2), 103–112. https://doi.org/10.1016/s0378-1119(00)00579-5

Timmons, L., & Fire, A. (1998). Specific interference by ingested dsRNA. *Nature*, *395*(6705), 854. https://doi.org/10.1038/27579

Wickham, H. (2016). *ggplot2: Elegant Graphics for Data Analysis*. Springer-Verlag. http://ggplot2.org

Wilkins, C., Dishongh, R., Moore, S. C., Whitt, M. A., Chow, M., & Machaca, K. (2005). RNA interference is an antiviral defence mechanism in Caenorhabditis elegans. *Nature*, *436*(7053), 1044–1047. https://doi.org/10.1038/nature03957

Wilson, R. C., & Doudna, J. A. (2013). Molecular Mechanisms of RNA Interference. *Annual Review of Biophysics*, *42*(1), 217–239. https://doi.org/10.1146/annurev-biophys-083012-130404

Winston, W. M., Sutherlin, M., Wright, A. J., Feinberg, E. H., & Hunter, C. P. (2007). Caenorhabditis elegans SID-2 is required for environmental RNA interference. *Proceedings of the National Academy of Sciences of the United States of America*, *104*(25), 10565–10570. https://doi.org/10.1073/pnas.0611282104

Wu, A. C.-Y., & Rifkin, S. A. (2015). Aro: A machine learning approach to identifying single molecules and estimating classification error in fluorescence microscopy images. *BMC Bioinformatics*, *16*, 102. https://doi.org/10.1186/s12859-015-0534-z

Wynant, N., Santos, D., & Vanden Broeck, J. (2017). The evolution of animal Argonautes: Evidence for the absence of antiviral AGO Argonautes in vertebrates. *Scientific Reports*, *7*(1), 9230. https://doi.org/10.1038/s41598-017-08043-5

Yigit, E. (2007). *The Argonaute Family of Genes in Caenorhabditis Elegans: A Dissertation*. University of Massachusetts Medical School.

Yigit, E., Batista, P. J., Bei, Y., Pang, K. M., Chen, C.-C. G., Tolia, N. H., Joshua-Tor, L., Mitani, S., Simard, M. J., & Mello, C. C. (2006). Analysis of the C. elegans Argonaute Family Reveals that Distinct Argonautes Act Sequentially during RNAi. *Cell*, *127*(4), 747–757. https://doi.org/10.1016/j.cell.2006.09.033

Youngman, E. M., & Claycomb, J. M. (2014). From early lessons to new frontiers: The worm as a treasure trove of small RNA biology. *Frontiers in Genetics*, *5*, 416. https://doi.org/10.3389/fgene.2014.00416

SUPPLEMENT

Contents

Figure S1. Embryonic lethality following RNAi against *par-1* in the *ppw-1;peel-2* mutant

Figure S2. Complementation test for DL238 with pooled hermaphrodites

Figure S3. RNAi against germline-expressed GFP in wild-type strains

Figure S4. RNAi sensitivity for 55 wild isolates versus genetic distance from reference strain N2

Figure S5. Droplet digital PCR results for *ppw-1* and *sago-2* for all ten tested strains

Figure S6. Population-level sequence variation for 62 RNAi genes

Table S1. Statistical estimates for changes in smFISH transcript abundance

Table S2. Statistical results for the ddPCR analysis

Table S3. Candidate genes for weak germline RNAi in the seven strains tested

Table S4. Strains used in this study

File S1. Statistical details of smFISH in early stage embryos

File S2. Details of genetic incompatibilities

File S3. Sequences of *ppw-1* and *sago-2* in CB4856, N2 and QX1211 (see attached file)

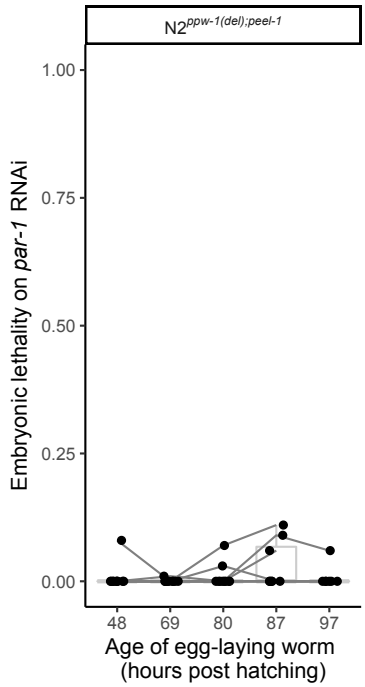

Figure S1. Embryonic lethality following RNAi against *par-1* in the *ppw-1;peel-2* mutant.

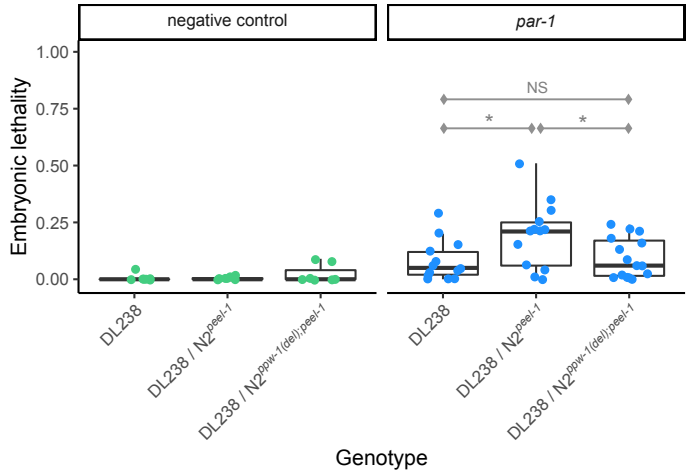

Figure S2. Complementation test for DL238 with pooled hermaphrodites. DL238 was crossed to the RNAi-sensitive laboratory strain N2, with and without a deletion allele at *ppw-1*. The embryos scored here were laid by pooled hermaphrodites on replicate plates. Significance level (Tukey's contrasts): $p<0.05$ (*).

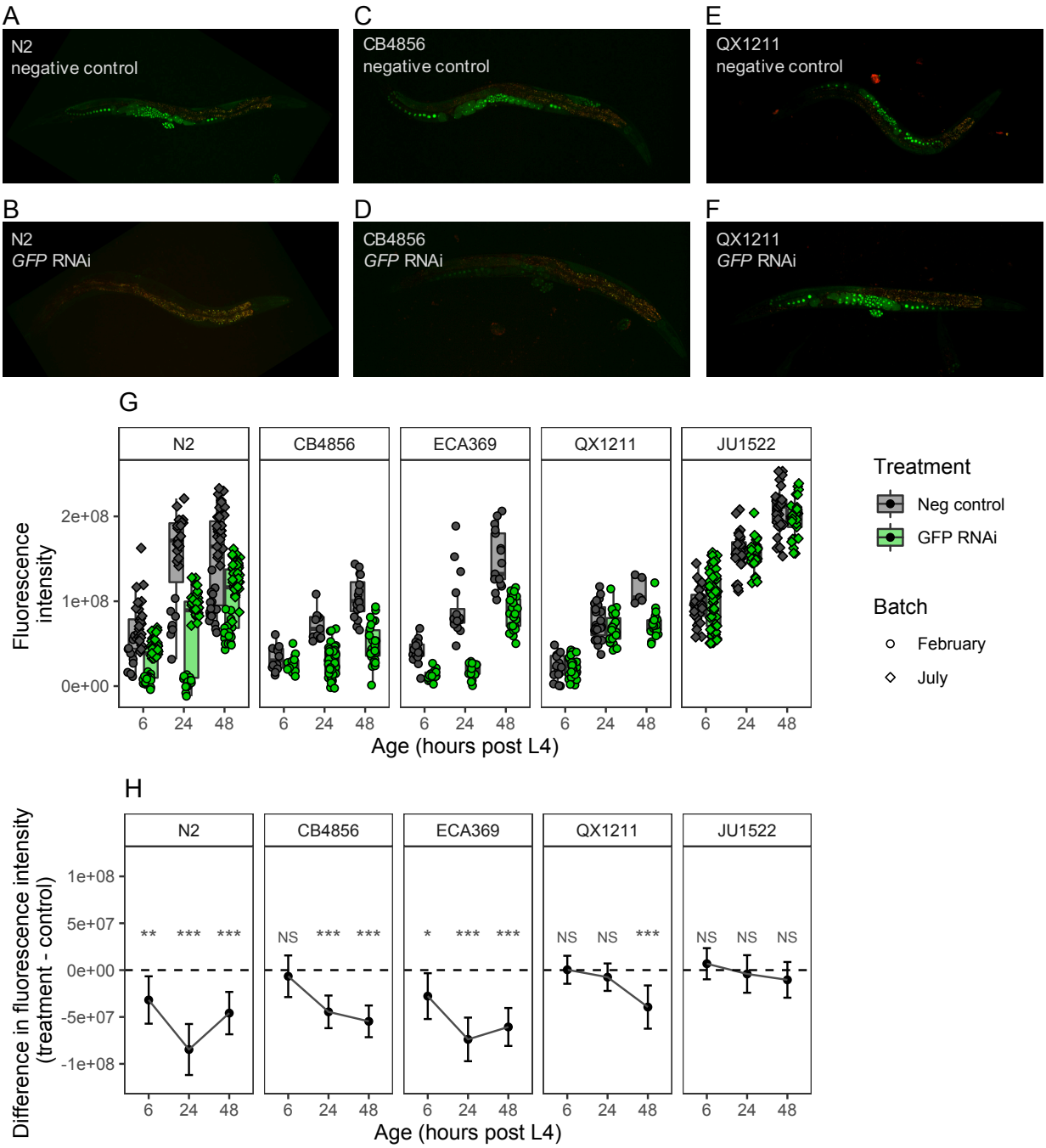

Figure S3. RNAi against germline-expressed GFP in wild-type strains. (A) - (F) Representative images of control and treated worms, all at 24hrs post L4 stage, are shown for N2, CB4856 and QX121. Green indicates GFP fluorescence; the red channel is overlaid on these images to show autofluorescence. (G) Whole-worm fluorescence intensity for worms imaged at 6, 24, and 48hrs post L4 stage; each point represents fluorescence measured for a single individual. (H) The difference in fluorescence intensity between treated and untreated samples; error bars represent standard error. Significance levels (Tukey's contrasts): $p<0.001$ (***), $p<0.01$ (**), $p<0.05$ (*).

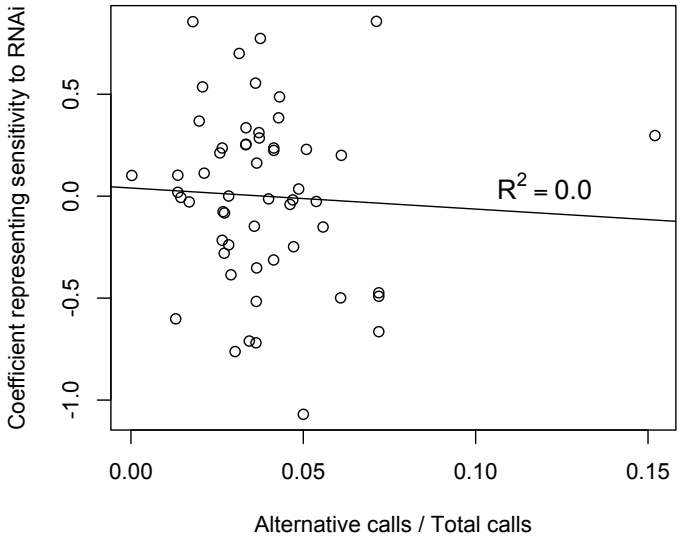

Figure S4. RNAi sensitivity for 55 wild isolates versus genetic distance from reference strain N2. RNAi data is from (*Paaby et al., 2015*), which measured embryonic lethality following RNAi by feeding against 29 individual maternal-effect targets. The y-axis plots the coefficients associated with the strain term in the full statistical model, and represents the strain-specific variation in embryonic lethality associated with RNAi responsiveness; increasingly positive values indicate weaker germline RNAi (*Paaby et al., 2015*). The x-axis gives the proportion of alternate genotype calls, out of the total number of calls, for each strain in the CeNDR database (*Cook et al., 2017*).

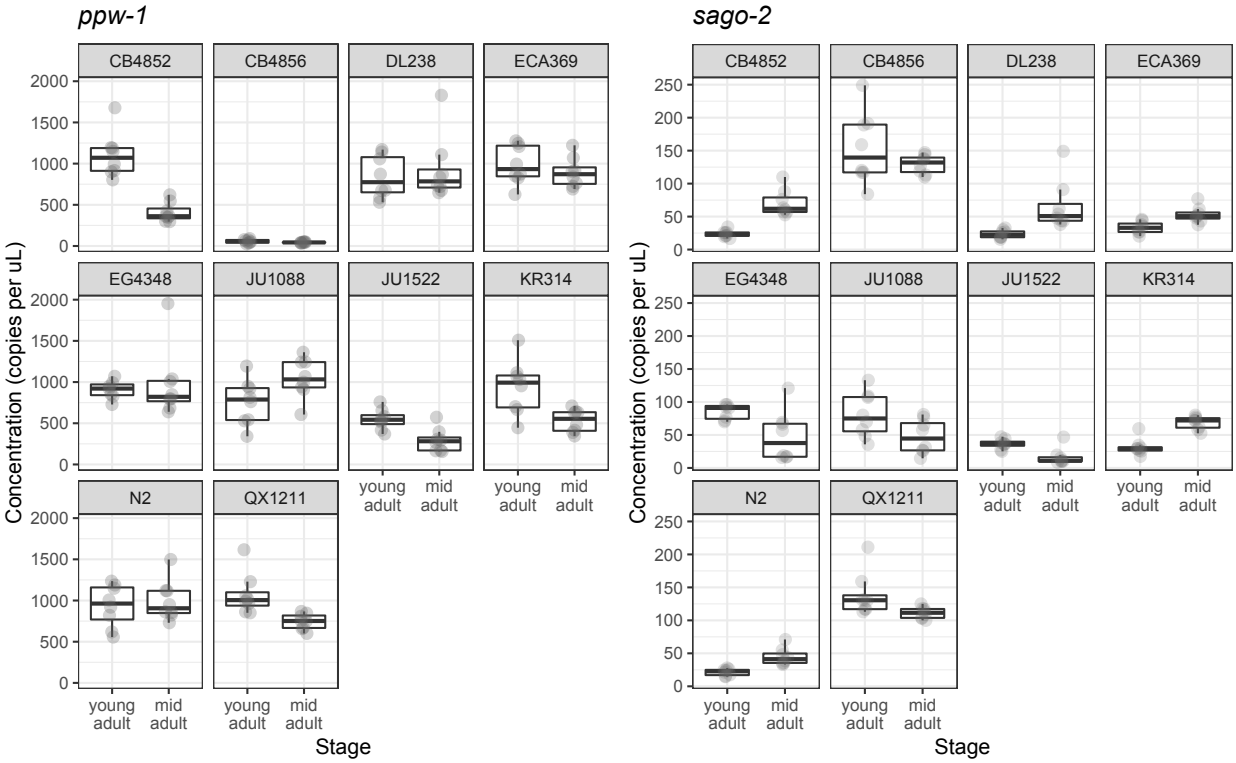

Figure S5. Droplet digital PCR results for *ppw-1* and *sago-2* for all ten tested strains.

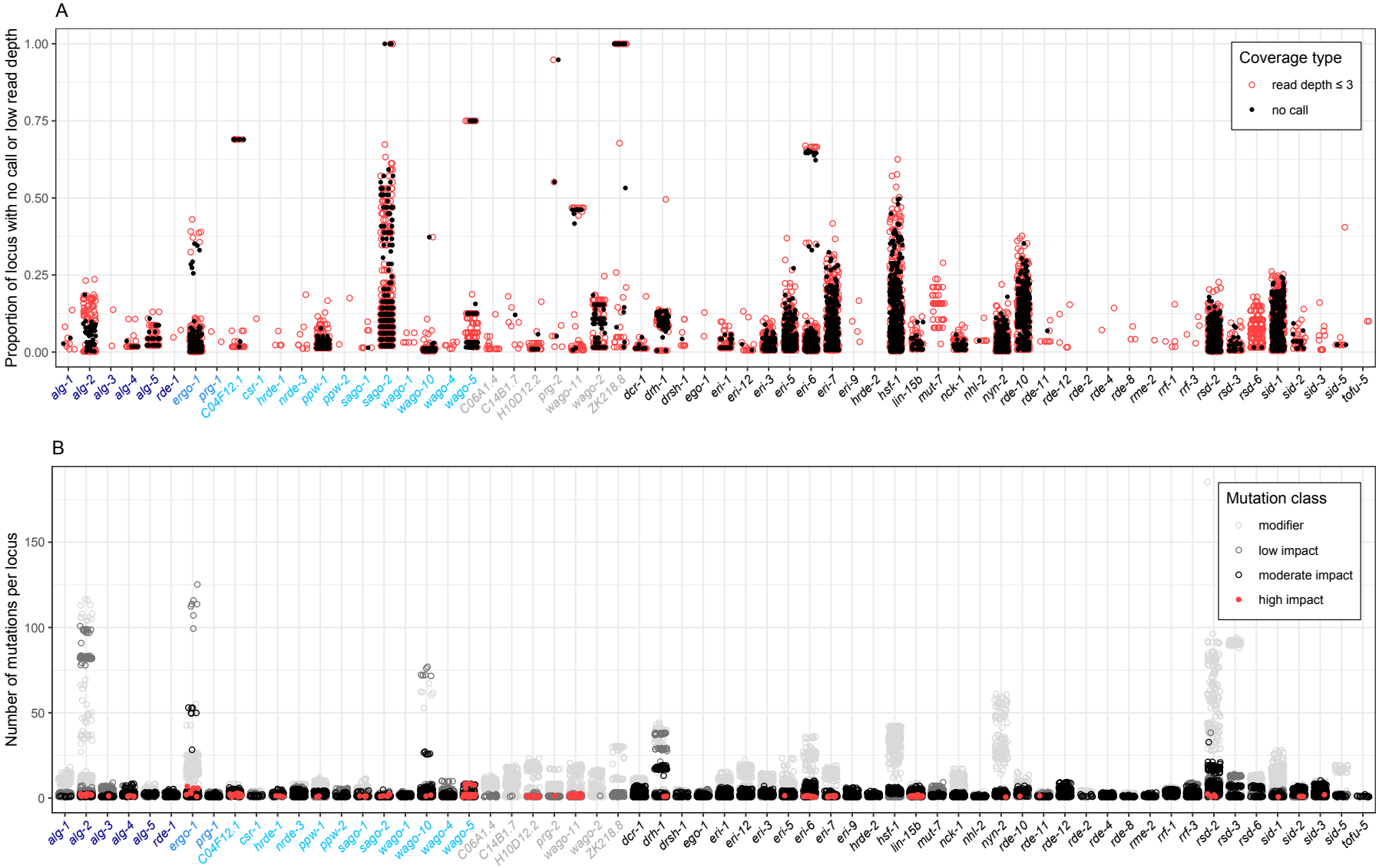

Figure S6. Population-level sequence variation for 62 RNAi genes. (A) mapping coverage and (B) mutational variation is shown for the 403 strain isotypes from CeNDR. Gene names are color coded by classification: AGO Argonaute (dark blue), PIWI Argonaute (blue), WAGO Argonaute (light blue), Argonaute pseudogene (grey), and other RNAi factor (black). Each point corresponds to an individual strain; zeros (no observation of poor coverage or mutation relative to the reference) are not plotted.

Table S1. Statistical estimates for changes in smFISH transcript abundance. The interaction term represents the changes in slope (Figure 2) between treated and untreated samples.

		Variance explained (ω^2)	p-value (ANCOVA model comparison)
N2	Treatment	0.586	<0.001
	Embryo stage	0.248	<0.001
	Interaction	0.059	<0.001
CB4856	Treatment	0.010	0.043
	Embryo stage	0.581	<0.001
	Interaction	0.017	0.012
QX1211	Treatment	0.014	0.037
	Embryo stage	0.208	<0.001
	Interaction	NA	NS

Table S2. Statistical results for the ddPCR analysis. The model used for each gene is described in the Methods.

ppw-1

	Df	Deviance	Resid. Df	Resid. Dev
NULL			158	37942
Strain	9	24433.1	149	13509
DevStage	1	910.3	148	12599
Strain:DevStage	9	4271.9	139	8327
Strain:DevStage:BiolRepl	20	2327.6	119	5999

sago-2

	Df	Deviance	Resid. DF	Resid. Dev
NULL			158	4722.0
RunDate	1	29.38	157	4692.6
Strain	9	2932.73	148	1759.9
DevStage	1	5.87	147	1754.0
Strain:DevStage	9	825.20	138	928.8
Strain:DevStage:BiolRepl	20	436.26	118	492.6

Table S3. Candidate genes for weak germline RNAi in the seven strains tested. Only genes with relevant genotypes in at least one strain are displayed, out of 62 RNAi genes queried. "High impact" indicates disruptive mutations like frameshifts or stop-gains. "Poor mapping coverage" indicates a read depth of 3 or less. "Functional diverged allele" indicates at least 1% nucleotide divergence from the reference genome, including at least five moderate mutations, such as amino acid substitutions, and no high impact mutations.

Class	Gene	One or more high impact mutation	Poor mapping coverage at 10% or more of locus	Functional diverged allele
Argonaute (AGO)	*alg-4*			QX1211
Argonaute (PIWI)	*ergo-1*	ECA369	ECA369	
Argonaute (WAGO)	*hrde-1*			QX1211
	nrde-3			QX1211
	ppw-1	CB4856		
	sago-2	DL238	DL238, ECA369, JU1522, KR314, QX1211	
	wago-10			QX1211
Argonaute (pseudogene)	*wago-11*	CB4852, KR314, QX1211	CB4856	
	wago-2		QX1211	
	ZK218.8		DL238	
Other RNAi factor	*dcr-1*			QX1211
	drh-1			QX1211
	eri-1			QX1211
	eri-5		JU1522	
	eri-6			QX1211
	eri-7	CB4856, DL238, ECA369	DL238, JU1522, KR314	
	eri-9			QX1211
	lin-15b	QX1211		ECA369
	nyn-2		DL238	QX1211
	rde-10		DL238, ECA369, JU1522, KR314, QX1211	
	rde-12			QX1211
	rsd-2		JU1522, QX1211	CB4856, DL238, ECA369, QX1211
	sid-1		DL238, ECA369, JU1522, QX1211	
	sid-2			QX1211
	sid-3			QX1211
	hsf-1		DL238, ECA369, JU1522, KR314	ECA369, KR314

Table S4. Strains used in this study.

Ref in text	Name	Genotype	Provenance
CB4852	CB4852	wild-type	Gift from Matthew Rockman
CB4856	CB4856	wild-type	Gift from Matthew Rockman
DL238	DL238	wild-type	Gift from Matthew Rockman
ECA369	ECA369	wild-type	Purchased from CeNDR
ECA701	ECA701	wild-type	Purchased from CeNDR
KR314	KR314	wild-type	Gift from Matthew Rockman
EG4348	EG4348	wild-type	Gift from Matthew Rockman
JU561	JU561	wild-type	Purchased from CeNDR
JU1088	JU1088	wild-type	Gift from Matthew Rockman
JU1522	JU1522	wild-type	Gift from Matthew Rockman
N2	N2	wild-type	Gift from Matthew Rockman
N2^{peel-1}	PTM377	*peel-1*(*kah126*) I	Gift from Patrick McGrath
N2^{ppw-1}	QF201	*ppw-1*(*pk1425*) I	Derived from backcrossing strain NL3511 5x to N2
N2$^{ppw-1;peel-1}$	QF204	*ppw-1*(*pk1425*) *peel-1*(*kah126*) I	Derived from PTM377 and QF201
N2$^{ppw-1\ CB4856}$	NL2550	*ppw-1*(*pk2505*) I	Purchased from CGC
NL3511	NL3511	*ppw-1*(*pk1425*) I	Purchased from CGC
QF14	QF14	*zuIs178*; *stIs10024 [RW10029>CB4856]*	Derived from backcrossing strain RW10029 18x to CB4856
QF15	QF15	*zuIs178; stIs10024 [RW10029>JU1522]*	Derived from backcrossing strain RW10029 16x to JU1522
QF16	QF16	*zuIs178*; *stIs10024 [RW10029>ECA369]*	Derived from backcrossing strain RW10029 17x to ECA369
QF90	QF90	*zuIs178*; *stIs10024 [RW10029>QX1211]*	Derived from backcrossing strain RW10029 10x to QX1211
QX1211	QX1211	wild-type	Gift from Matthew Rockman
RW10029	RW10029	*zuIs178*; *stIs10024*	Purchased from CGC
XZ1516	XZ1516	wild-type	Purchased from CeNDR

File S1. Statistical details of smFISH in early stage embryos

In early stage embryos (up to four cells), N2 showed a significant reduction in *par-1* transcript abundance after *par-1* RNAi ($t=-16.34$, $df=32$, $p<0.001$), while CB4856 and QX1211 did not ($t=0.41$, $df=56.31$, $p=0.684$ and $t=1.15$, $df=95.03$, $p=0.255$, respectively) (Figure 2D). However, for CB4856, the variance in abundance was slightly higher for treated embryos than for control embryos ($F=1.94$, $df=32,40$, $p=0.048$), which may represent the onset of an RNAi response. In QX1211, the variance of *par-1* treated embryos was substantially higher ($F=2.94$, $df=100,32$, $p<0.001$) and abundance was bimodally distributed, with low-abundance embryos at levels similar to N2; *par-4* treated embryos showed a slight reduction in average abundance and substantial increase in variance ($t=-2.64$, $df=24.20$, $p=0.014$ and $F=5.50$, $df=20,36$, $p<0.001$, respectively) (Figure 2D).

File S2. Details of genetic incompatibilities

C. elegans carries two known genetic incompatibilities: the paternally-delivered toxin *peel-1*, which is rescued by the zygotically-expressed antidote *zeel-1* (*Seidel et al., 2008, 2011*), and the maternally-delivered toxin *sup-35*, which is rescued by the zygotically-expressed antidote *pha-1 (Ben-David et al., 2017)*. In both instances, embryos that cytologically inherit the toxin but do not inherit the genotype to express the antidote will die. N2 carries both toxin-antidote complexes but several of our other wild isolates do not. Since our goal was to use embryonic lethality to measure the RNAi response, lethality arising from these genetic incompatibilities had the potential to confound our results.

To control for the *zeel-1;peel-1* incompatibility, we generated a strain derived from N2 with both the *ppw-1* deletion and an allele of *peel-1* (*kah126*) that disables the toxin by a frameshift insertion in the second exon ($N2^{ppw\text{-}1(del);peel\text{-}1}$). This allele eliminates embryonic lethality that would otherwise arise in the F2 generation, from F1 heterozygotes derived from incompatible strains. The presence of this *peel-1* allele had no effect on our measured RNAi response in either sensitive or resistant backgrounds (Figure 3A, Figure S1), so we used it in all comparisons requiring the N2 background.

We did not control for the *sup-35;pha-1* incompatibility. We anticipated toxin-associated embryonic lethality to occur from crosses initiated between N2 and two wild isolates without the active *sup-35;pha-1* complex: DL238 and QX1211. For DL238, we observed only very weak penetrance of this effect (Figure 3C). For QX1211, we observed clear toxin-associated lethality, as embryos derived from the N2 × QX1211 cross showed lethality on the control condition (Figure 3D). However, we were still able to infer a distinct *ppw-1*-associated response in this assay, as lethality from the QX1211/$N2^{peel\text{-}1}$ genotype matched that of the control and lethality from QX1211/$N2^{ppw\text{-}1(del);peel\text{-}1}$ was significantly higher (Figure 3D).